Title
Finite Element Formulations for Problems of Finite Deformation of Elasto-Viscoplastic Beams

Authors
Simo, Juan
Hjelmstad, Keith
Taylor, Robert

Publication Date
1983

REPORT NO.
UCB/SESM-83/01

STRUCTURAL ENGINEERING AND
STRUCTURAL MECHANICS

FINITE ELEMENT FORMULATIONS FOR PROBLEMS OF FINITE DEFORMATION OF ELASTO-VISCOPLASTIC BEAMS

by

JUAN C. SIMO

KEITH D. HJELMSTAD

ROBERT L. TAYLOR

JANUARY 1983

DEPARTMENT OF CIVIL ENGINEERING
UNIVERSITY OF CALIFORNIA
BERKELEY, CALIFORNIA

Finite Element Formulations for Problems of Finite Deformation of Elasto-Viscoplastic Beams

By

Juan C. Simo

Keith D. Hjelmstad

and

Robert L. Taylor

Structural Engineering and Structural Mechanics
Department of Civil Engineering
University of California, Berkeley
Berkeley, California

FINITE ELEMENT FORMULATIONS FOR PROBLEMS OF FINITE DEFORMATION OF ELASTO-VISCOPLASTIC BEAMS

J. C. SIMO.

K. D. HJELMSTAD

R. L. TAYLOR

Department of Civil Engineering. University of California, Berkeley.

1.- INTRODUCTION

We consider in this paper problems involving finite deformation of elasto-viscoplastic beams from a numerical standpoint, with special emphasis on the effect of shear deformation. In treating these problems two alternative approaches may be followed. One can directly employ the three dimensional theory without taking advantage of the particular geometry of the body. Or, alternatively, one can exploit the simple aspects of the geometry involved by introducing a kinematic assumption to constrain the general (three dimensional) theory, and thereby develop a restricted (more tractable) theory in a systematic way. Here we will follow the latter approach, the success of which clearly depends upon the nature of the kinematic assumption. In the context of the non-linear theory, the formal use of generalized projection methods have been proposed by Antman [1] to consistently develop kinematics assumptions.

By far the most widely used kinematic constraint is the assumption that cross sections normal to the line of centroids in the undeformed configuration remain plane in the deformed configuration. Under this assumption, shear deformation can be approximately taken into account by decoupling the rotation of the cross section from the slope of the deformed line of centroids. Although fully non-linear theories can be developed on the basis of this assumption [1,2,3], they are incapable of reproducing the exact solution of the (linear) Saint Venant's problem [5], a test proposed by Novozhilov [1, references therein] as an assessment of the accuracy of a beam theory. Within the framework of the linear theory and based on early work of Cowper [6],a kinematic assumption was developed by Simo [3] which renders the exact solution of Saint Venant's problem. The two kinematic assumptions described above are employed in this paper and the resulting theories are compared.

From a numerical point of view, two approaches may be followed within the scope of formulations restricted by a kinematic constraint. One can directly implement each theory entirely formulated in terms of stress resultants and their conjugate strain measures. Alternatively, one can use the kinematic constraint in conjunction with the the three dimensional field equations to obtain a one dimensional formulation by *numerically integrating* the equations over the cross section of the beam. In this paper we shall consider the numerical implementation of both approaches, and compare their performances through an extensive set of examples.

In the stress resultant approach the following topics are examined:

(i) We first consider a simple fully non-linear stress resultant formulation, proposed in [3], capable of modeling finite stretching, shearing and bending of a beam. This formulation, which employs the "plane sections" hypothesis is used to exhibit the methodology and is subsequently compared with a second order approximation to the three dimensional non-linear theory, in terms of stress resultants, developed in [4], which accounts for transverse warping of the cross section of the beam.

(ii) The formulation discussed in (i), is then extended to treat the elasto-viscoplastic problem. Such an extension involves the development of an objective rate of change of stress resultants, together with the formulation of an appropriate plastic flow potential in order to characterize the inelasticity of the material.

(iii) The numerical treatment of the problem is accomplished by first integrating the time dependence of the non-linear constitutive equations using the unconditionally stable scheme proposed by Hughes and Taylor [7]. However, our approach differs from that proposed in [7] in that the non-linear equations that result from the time integration are exactly satisfied at the *local* level within each *global* iteration of each time step.

The main drawback of an inelastic, stress resultant beam theory is the way in which the inelasticity is manifested. The use of a plastic flow potential, while technically correct, has the disadvantage that processes which are local to the cross section, such as the propagation of an elastic-plastic interface, cannot be captured. Furthermore, for many cross sectional geometries of interest it is difficult to obtain any reasonable expression for the potential.

(iv) The limitations of the stress resultant formulations are partially overcome by employing the procedure of numerical integration over the cross section as previously described. The displacement field developed in [3], which is exact for Saint Venant's problem, is employed as the kinematic constraint.

This approach, while maintaining some of the simple features of a one dimensional theory, is capable of rendering information at a local level. Previous attempts in this direction have employed the "plane sections" hypothesis [8] *which is inadequate to treat problems involving high shear* since the constant distribution of shear stresses obtained from this hypothesis precludes the propagation of an elastic-plastic interface from the middle fibers of the beam. Several numerical examples, presented in Section 4., illustrate this point.

The approach of numerically integrating over the cross section permits the consideration of general three dimensional constitutive models which are difficult, if not impossible, to realize in a stress resultant formulation. In particular, the model linearly relating the second Piola-Kirchhoff stress tensor to the Lagrangian strain tensor, which is widely used both for computational purposes and in the derivation of approximate nonlinear stress resultant models [†] is implemented in Example 5. The example suggests that this relationship may lead to results of questionable physical significance.

2.- STRESS RESULTANT FORMULATION

Throughout this paper, we consider an initially straight rod of length L with cross section $\Omega \subset \mathbb{R}^2$, a bounded open set with smooth boundary $\partial\Omega$. Prior to the formulation of the equilibrium equations in terms of stress resultants, we shall examine some geometric notions involved in a formulation of the field equations suitable for the consideration of the effect of shear. Appropriate constitutive equations in terms of the stress resultants will be considered later.

2.1.- Kinematic Considerations.

Our notation is summarized as follows. Coordinates in the reference configuration $B \equiv (0,L)\times\Omega$ are designated by $\{X^I\}$ with coordinate vector fields $\{\hat{\mathbf{E}}_I\}$ taken to be the standard basis in $\mathbb{R}^3$. $\{X^2, X^3\}$ are assumed to be principal axes of inertia of Ω. The fixed spatial coordinate system $\{x^i\}$ with associated basis $\{\hat{\mathbf{e}}_i\}$ is taken as collinear with $\{X^I\}$. Although $\{\hat{\mathbf{e}}_i\} \equiv \{\hat{\mathbf{E}}_I\}$, it will prove convenient to maintain the notational distinction. The deformation map is denoted by $\boldsymbol{\phi} : B \subset \mathbb{R}^3 \to \mathbb{R}^3$. Points in B are designated by X and points in the deformed configuration $\boldsymbol{\phi}(B)$ by x. Following standard practice, the deformation gradient is designated by $\mathbf{F}(X) = \dfrac{\partial\boldsymbol{\phi}}{\partial\mathbf{X}}$. In addition, if $\{\theta^I\} = \{X^I \circ \boldsymbol{\phi}^{-1}\}$ is the convected coordinate system covering $\boldsymbol{\phi}(B) \subset \mathbb{R}^3$, the convected coordinate vector fields may be defined as [9] $\mathbf{l}_I(x) = \mathbf{F}\hat{\mathbf{E}}_I \circ \boldsymbol{\phi}^{-1}(x)$, for any $x = \boldsymbol{\phi}(X)$. By a slight abuse of notation, $X \in B$ and $x \in \boldsymbol{\phi}(B)$ will be identified by their position vectors $\mathbf{X}$ and $\mathbf{x}$.

[†] See, for example, Ciarlet [30].

Consider an arbitrary cross section Ω at any $X^1 \in (0, L)$ regarded as fixed. The deformed cross section $\phi(\Omega)$ is then a surface in $\mathbb{R}^3$ defined by the map $\phi|_{X^1=Fixed} : \Omega \rightarrow \mathbb{R}^3$ thereby parametrized by the material coordinates (X^2, X^3). At each $\mathbf{x} \in \phi(\Omega)$, the vector fields $\mathbf{l}_\Gamma \circ \phi|_{X^1=Fixed}$ are tangent to the coordinate lines on $\phi(\Omega)$ obtained by setting $X^\Gamma = Constant$ (Γ=2,3) and, therefore, tangent to $\phi(\Omega)$. In addition, we introduce the vector field $\mathbf{n}(\mathbf{X})$ [†] normal to $\phi(\Omega)$ at $\mathbf{x}$, and given by $\hat{\mathbf{n}}(\mathbf{X}) = J\,\mathbf{F}^{-T}\hat{\mathbf{E}}_1$. Denoting by $\mathbf{C} = \mathbf{F}^T\mathbf{F}$ is the right Cauchy-Green tensor, the frame composed by the unit vector fields $\{\hat{\mathbf{g}}_i\}$ defined by

$$\hat{\mathbf{g}}_1 \equiv \frac{\mathbf{n}(\mathbf{X})}{||\mathbf{n}||} \equiv \left(\frac{d\omega}{d\Omega}\right)^{-1} J\mathbf{F}^{-T}|_{X^1=Fixed}\cdot\hat{\mathbf{E}}_1$$

$$\mathbf{g}_\Gamma \equiv \frac{\mathbf{l}_\Gamma(\mathbf{X})}{||\mathbf{l}_\Gamma||} = \frac{1}{\sqrt{C_{\Gamma\Gamma}}}\mathbf{F}(\mathbf{X})|_{X^1=Fixed}\hat{\mathbf{E}}_\Gamma \qquad (no\ sum\ on\ \Gamma=2,3) \tag{1}$$

characterizes the local geometry of the deformed cross section $\phi(\Omega)$ and is often referred to as *Gaussian* or *intrinsic* frame in the context of differential geometry [10]. This frame plays a key role in the subsequent developments. Its relationship to the fixed spatial frame $\{\hat{\mathbf{e}}_i\}$ will be written as

$$\{\hat{\mathbf{g}}_i\} = \mathbf{\Lambda}^T(\mathbf{X})\ \{\hat{\mathbf{e}}_i\} \tag{2}$$

For coplanar problems, for example, where $g_3 \equiv \hat{\mathbf{e}}_3$, the transformation $\mathbf{\Lambda}$ may be defined as [3,4]

$$\mathbf{\Lambda}(\psi(\mathbf{X})) = \begin{bmatrix} \cos\psi & -\sin\psi & 0 \\ \sin\psi & \cos\psi & 0 \\ 0 & 0 & 1 \end{bmatrix} \tag{3}$$

where $\psi(\mathbf{X}) \equiv -\dfrac{F_1^2(\mathbf{X})}{F_2^2(\mathbf{X})}$ depends, in general, upon X^1, and X^2.

A systematic procedure for developing rod theories employs the general three dimensional theory as the point of departure and subsequently constraints the position vector $\mathbf{x}$ of particles x in the deformed configuration by introducing a kinematic hypothesis. Clearly, the resulting restricted theory depends upon the nature of the assumed kinematic constraint. Following this procedure, we discuss kinematic assumptions suitable for the consideration of the effect of shear.

The "Plane Sections Remain Plane" Assumption. Consider the classical hypothesis stating that *plane sections normal to the line of centroids remain plane after deformation.* In accordance

[†] Strictly speaking, $\hat{\mathbf{n}}$ is a one-form. Our choice of coordinates makes the distinction irrelevant.

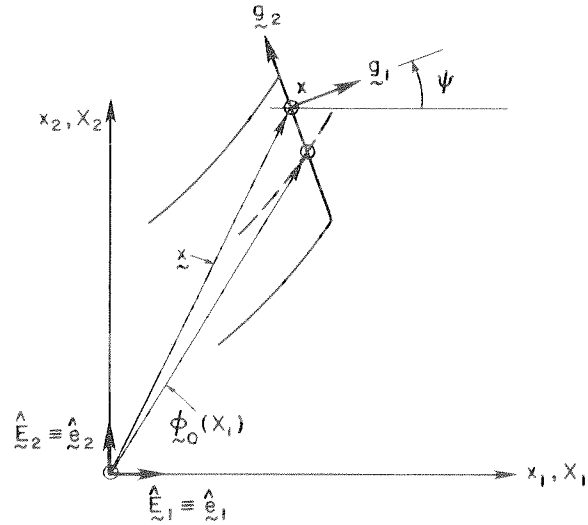

Fig. 1. Kinematic assumption, ignoring the effect of transverse warping.

with this assumption, the *Gaussian* ("moving") frame $\{\hat{g}_i\}$ is independent of the transverse coordinates and thus its orientation remains invariant on any (deformed) cross section $\phi(\Omega)$. For coplanar systems, the deformation map then takes the form

$$\boldsymbol{\phi}(\mathbf{X}) = \boldsymbol{\phi}_o(X^1) + X^2\,\hat{\mathbf{g}}_2(X^1) \tag{4a}$$

where $\boldsymbol{\phi}_o = \boldsymbol{\phi}(\mathbf{X})\big|_{X^2=0}$, the position vector of the line of centroids in the deformed configuration, and $\hat{\mathbf{g}}_2(X^1)$ are expressed as (Fig. 1)

$$\begin{aligned} \boldsymbol{\phi}_o(X^1) &= (X^1 + u(X^1))\hat{\mathbf{e}}_1 + v(X^1)\hat{\mathbf{e}}_2 \\ \hat{\mathbf{g}}_2(X^1) &= -\sin\psi(X^1)\hat{\mathbf{e}}_1 + \cos\psi(X^1)\hat{\mathbf{e}}_2 \end{aligned} \tag{4b}$$

For future reference, note that as a result of (4) we have the expressions

$$\begin{aligned} J_o &\equiv \det(\mathbf{F})\big|_{X^2=0} = (1+u')\cos\psi + v'\sin\psi \\ C_{12} &\equiv \hat{\mathbf{E}}_2 . (\mathbf{C}\hat{\mathbf{E}}_1) = -(1+u')\sin\psi + v'\cos\psi \end{aligned} \tag{5}$$

Assumption (4) allows for arbitrarily large rotations, shearing, and extension of the beam. However, this kinematic assumption completely ignores the transverse warping of the cross section of the beam, which necessarily appears as a result of shear deformation, and hence leads to a restricted theory which is incapable of reproducing the exact solution of Saint-Venant's problem. To examine the effect of transverse warping we restrict our attention momentarily to the linear theory.

The Exact Linearized Kinematics for Saint-Venant's Problem. Based upon the solution for Saint-Venant's problem, it is possible to formulate a more elaborate kinematic assumption which accounts for the effect of transverse warping. As shown in [3], the *exact* linearized kinematics for this problem may be expressed as an expansion of the form

$$\begin{aligned} u^1(\mathbf{X}) &= \bar{u}(X^1) - X^2\bar{\psi}(X^1) - \kappa\Phi_1(X^2,X^3)\bar{\beta}(X^1) \\ u^2(\mathbf{X}) &= \bar{v}(X^1) + \nu\Phi_2(X^2,X^3)\bar{\psi}'(X^1) - \nu X^2\bar{u}'(X^1) \\ u^3(\mathbf{X}) &= \nu\Phi_3(X^2,X^3)\bar{\psi}'(X^1) - \nu X^3\bar{u}'(X^1) \end{aligned} \tag{6}$$

where the kinematic variables $\{\bar{u},\ \bar{v},\ \bar{\psi},\ \bar{\beta}\}$ are defined by

$$\begin{aligned} \bar{u}(X^1) &= \frac{1}{\Omega}\int_\Omega u^1(\mathbf{X})\,d\Omega; \qquad & \bar{v}(X^1) &= \frac{1}{\Omega}\int_\Omega u^2(\mathbf{X})\,d\Omega \\ \bar{\psi}(X^1) &= \frac{1}{I_2}\int_\Omega X^2u^1(\mathbf{X})\,d\Omega; \qquad & \bar{\beta} &\equiv \bar{v}' - \bar{\psi}. \end{aligned} \tag{7}$$

The coordinate functions $\Phi_i(X^2,X^3)$, $(i=1,2,3)$ can be expressed in terms of Love's flexure function [5] $\chi : \Omega \to \mathbb{R}$ as [3]

$$\begin{aligned} \Phi_1 &\equiv \frac{\Omega}{2(1+\nu)I_2}\left\{\chi + X^2(X^3)^2 - \frac{1}{\Omega}\int_\Omega [\chi + X^2(X^3)^2]\,d\Omega - \frac{X^2}{I_2}\int_\Omega [\chi + X^2(X^3)^2]X^2\,d\Omega\right\} \\ \Phi_2 &\equiv \frac{1}{2}\left\{(X^2)^2 - (X^3)^2 - \frac{I_2 - I_3}{\Omega}\right\} \\ \Phi_3 &\equiv X^2X^3 \end{aligned} \tag{8}$$

where $I_\alpha \equiv \int_\Omega (X^\alpha)^2 d\Omega$ are the principal moments of inertia, ν is Poisson's ratio, and the coefficient κ may be defined in terms of $\Phi_1 : \Omega \to \mathbb{R}$ as

$$\kappa = \frac{1}{1 + \dfrac{1}{\Omega}\displaystyle\int_\Omega \frac{\partial\Phi_1}{\partial X^2}\,d\Omega} \tag{9}$$

and can be shown to correspond to the expression for the shear coefficient first derived by Cowper [6]. An explicit expression for $\mathbf{\Lambda}$ consistent with (6), now depending upon the transverse coordinates X^2, X^3, can be found in [4]. This explicit dependence upon the transverse coordinates occurs as a result of the warping and Poisson's effects.

The kinematics (6) may be regarded as an expansion resulting from the application of the projection method due to Kantorovich [11] in terms of coordinate functions which are L^2–orthogonal over Ω. Such an expansion is optimal in the sense that it is capable of reproducing the exact stress solution corresponding to Saint-Venant's problem [3,4]. Based upon (6) an exact second order solution to Saint-Venant's problem within the framework of three dimensional nonlinear elastostatics was derived in [4] by means of the method of successive approximations.

In the next section we formulate the local form of the equilibrium equations in terms of stress resultants, based upon both assumptions (4) and (6). The implications of each assumption are discussed.

2.2.- Equilibrium Equations. Local Form.

The equilibrium equations of the non-linear theory may be expressed in terms of the first Piola-Kirchhoff stress tensor as

$$DIV\ \mathbf{P}(\mathbf{X}, \nabla\boldsymbol{\phi}) + \rho_{ref}\mathbf{B}(\mathbf{X}) = 0\ , \qquad \mathbf{F}\,\mathbf{P}^T = \mathbf{P}\,\mathbf{F}^T \tag{10}$$

For an arbitrary cross section Ω, the resultant force $\mathbf{R}(X^1)$ and moment $M(X^1)$ acting on $\boldsymbol{\phi}(\Omega)$ are given by (summation convention is implied)

$$\mathbf{R} = \int_\Omega \mathbf{P}\ \hat{\mathbf{E}}_1\, d\Omega \equiv R_x^i\, \hat{\mathbf{e}}_i \qquad M = \hat{\mathbf{e}}_3 . \int_\Omega (\boldsymbol{\phi}(\mathbf{X}) - \mathbf{x}_o) \times \mathbf{P}\ \hat{\mathbf{E}}_1\, d\Omega \tag{11}$$

where $\mathbf{x}_o = \boldsymbol{\phi}(\mathbf{X})\,|_{X^2=0}$. The prescribed forces acting on the rod are assumed to be contained in the plane of symmetry X^1–X^2 of the rod and thus $R_x^3 \equiv 0$. If one neglects the effect of transverse warping then $\boldsymbol{\Lambda}(\psi)$, as given by (3), is independent of the transverse coordinates X^2, X^3 and it trivially follows that $\{R_x^i\} = \boldsymbol{\Lambda}(\psi)[N\ \ V\ \ 0]^T$, where $\mathbf{R} = N\hat{\mathbf{g}}_1 + V\hat{\mathbf{g}}_2$. It can then be shown [3] that the counterpart of equations (10) in terms of the normal and tangential stress resultants N and V respectively, takes the form

$$\frac{d}{dX^1}\left\{\boldsymbol{\Lambda}(\psi)\begin{Bmatrix} N \\ V \\ 0 \end{Bmatrix}\right\} + \begin{Bmatrix} p(X^1) \\ q(X^1) \\ 0 \end{Bmatrix} = 0$$

$$\frac{dM}{dX^1} + J_o V - C_{12} N = 0. \tag{12}$$

where $\mathbf{t}(X^1) = p(X^1)\hat{\mathbf{e}}_1 + q(X^1)\hat{\mathbf{e}}_2$ are the transversally applied forces. For simplicity, we assume $p(X^1) \equiv 0$ in the sequel.

Using (6) as a point of departure, it is possible to develop a second order approximation to the nonlinear equations (10) in terms of stress resultants N, V, M. However, due to the dependence of $\mathbf{\Lambda}$ on the transverse coordinates this development requires some further results. Here, we state the final result and refer the reader to [4] for details of the derivation.

$$
\begin{aligned}
[N - \bar{\psi}\, V]' &= 0 \\
[V + (1-\kappa)\,(\bar{v}' - \bar{\psi})\, N]' &= 0 \\
M' + (1 + \bar{u}')\, V - \kappa\,(\bar{v}' - \bar{\psi})\, N &= 0
\end{aligned}
\tag{13}
$$

Making use of (5) one can easily develop a second order approximation to the equilibrium equations (12) based upon assumption (4) which ignores the effect of transverse warping. Comparing this result with the second order equilibrium equations (13), the following conclusions are obtained [3]

(i) As a result of the effect of transverse warping, the additional term $(1-\kappa)\,(\bar{v}' - \bar{\psi})\, N$ appears in $(13)_2$. The physical interpretation of this result is that the resultant N of normal stresses acting on $\phi(\Omega)$ no longer remains normal to the (average) plane of bending defined by the angle $\bar{\psi}(X^1)$.

(ii) The second order approximation to the last term in $(12)_2$ differs from the corresponding term in $(13)_3$ by a factor κ, which again is the result of the transversal warping effect.

Conclusions (i) and (ii) show that restricted rod theories based upon either the approximate kinematic hypothesis which ignores the effect of transverse warping (4) or, alternatively, on the exact displacement field for Saint-Venant's problem (6), lead to different expression of the second order equilibrium equations in terms of stress resultants. Numerical examples are presented in section 4. which illustrate these differences. In the rest of this section, equations (12) are employed in the development of our formulation in terms of stress resultants. The details of stress resultant formulation employing the kinematics (6) and equilibrium equations (13) parallels the development that follows and can be found in [3,4].

2.3.- Equilibrium Equations. Weak Form.

The following notation is introduced for convenience and employed in the following development.

$$\mathbf{w} = [(X^1 + u(X^1)) \quad v(X^1) \quad \psi(X^1)]^T$$

$$\mathbf{R}_x = [R^1 \;\; R^2 \;\; M]^T \qquad \mathbf{R}_g = [N \;\; V \;\; M]^T \tag{14a}$$

The set of components $\mathbf{R}_x$ and $\mathbf{R}_g$ with respect to the spatial and Gaussian frames are related by $\mathbf{R}_x = \boldsymbol{\Lambda}(\psi)\, \mathbf{R}_g$. In addition, we introduce the linear operator $\mathbb{F} : [H^1(0, L)]^3 \to [L^2(0, L)]^3$ defined by

$$\mathbf{w} \to \mathbb{F}(\mathbf{w}) = [(1+u') \quad v' \quad \psi']^T \tag{14b}$$

where a "prime" designates d/dX^1. To further simplify the notation, let us designate by $\partial_{\mathbf{w}}$ the directions at either $X^1 = 0$ or $X^1 = L$ along which some or all the components of $\mathbf{w}$ are prescribed to values designated by $\tilde{\mathbf{w}}$. Similarly, $\partial_{\mathbf{R}}$ will designate the directions at $X^1 = 0,\ L$ along which entries in $\mathbf{R}_x$ are prescribed to have values $\tilde{\mathbf{R}}_x$. We require $\partial_{\mathbf{w}} \bigcap \partial_{\mathbf{R}} = \emptyset$. The linear space of kinematically admissible variations (test functions) may then be defined as

$$W = \{\, \boldsymbol{\eta} \in [H^1(0, L)]^3 \mid \quad \boldsymbol{\eta}|_{\partial_{\mathbf{w}}} = 0 \} \tag{15}$$

The equilibrium equation $(12)_2$ for the bending moment M can, in view of (5), be written as

$$-\frac{dM}{dX^1} + \mathbb{F}^T(\mathbf{w}).\frac{d\boldsymbol{\Lambda}^T}{d\psi}(\psi).\mathbf{R}_g = 0 \tag{16}$$

Combining (16) with the equilibrium equation $(12)_1$ for the components N and V of the resultant force $\mathbf{R}$, the weak form of the equilibrium equations takes the form

$$G(\boldsymbol{\eta},\mathbf{w}) = \int_0^L \mathbf{R}_g.[\,\boldsymbol{\Lambda}^T(\psi)\mathbb{F}(\boldsymbol{\eta}) + \eta_3\frac{d\boldsymbol{\Lambda}^T}{d\psi}(\psi)\mathbb{F}(\mathbf{w})]\ dX$$

$$-\int_0^L q(X^1)\eta_2(X^1)\ dX - [\boldsymbol{\eta}.\tilde{\mathbf{R}}_x]_{\partial_{\mathbf{R}}} = 0\,, \quad \text{for } \textit{any} \quad \boldsymbol{\eta} \in W \tag{17}$$

Upon defining

$$\boldsymbol{\lambda}_g(\mathbf{w}) = \boldsymbol{\Lambda}^T(\psi)\begin{Bmatrix} 1+u'-\cos\psi \\ v'-\sin\psi \\ \psi' \end{Bmatrix} \equiv \boldsymbol{\Lambda}^T(\psi)[\mathbb{F}(\mathbf{w}) - \hat{\mathbf{n}}] \tag{18}$$

where $\hat{\mathbf{n}}(X^1)$ is given by (3), the weak form (17) can be written as

$$G(\boldsymbol{\eta},\mathbf{w}) = \int_0^L \mathbf{R}_g.D\boldsymbol{\lambda}_g(\mathbf{w}).\boldsymbol{\eta}\ dX - \int_0^L q\,\eta_2 dX - [\boldsymbol{\eta}.\tilde{\mathbf{R}}_x]_{\partial_{\mathbf{R}}} = 0\,, \quad \text{for } \textit{any} \quad \boldsymbol{\eta} \in W \tag{19}$$

where $D\boldsymbol{\lambda}_g(\mathbf{w}).\boldsymbol{\eta}$ is defined in the usual manner as

$$D\boldsymbol{\lambda}_g(\mathbf{w}).\boldsymbol{\eta} = \frac{d}{d\alpha}[\boldsymbol{\Lambda}^T(\psi+\alpha\eta_3)\mathbb{F}(\mathbf{w}+\alpha\boldsymbol{\eta})]_{\alpha=0} \tag{20}$$

We therefore conclude that $\boldsymbol{\lambda}_g(\mathbf{w})$, as defined by (18), are the measures of deformation dual to the generalized forces $\mathbf{R}_g$.

Remarks

(i) Since $\boldsymbol{\lambda}_g(\mathbf{w})$ are the strain measures associated with $\mathbf{R}_g$, and $\mathbf{R}_x = \boldsymbol{\Lambda}(\psi)\mathbf{R}_g$, equation (18) shows that $[\mathbb{F}(\mathbf{w}) - \hat{\mathbf{n}}]$ are the strain measures associated with the components $\mathbf{R}_x$. Obviously, $[\mathbb{F}(\mathbf{w}) - \hat{\mathbf{n}}]$ and $\boldsymbol{\lambda}_g$ define the same object $\boldsymbol{\lambda}$ in different coordinate systems.

(ii) $\boldsymbol{\lambda}_g$ admits a simple geometrical interpretation. The stretching of the line of centroids is given by

$$\boldsymbol{\delta} \equiv \mathbf{F}\big|_{X^2=0}\hat{\mathbf{E}}_1 = (1+u')\hat{\mathbf{e}}_1 + v'\hat{\mathbf{e}}_2 \tag{21}$$

The axial stretching in the normal direction $\hat{\mathbf{n}} \equiv \hat{\mathbf{g}}_1$ and the shearing in the tangential direction $\hat{\mathbf{g}}_2$ then have the expressions

$$\begin{aligned} \delta_n &\equiv \boldsymbol{\delta}.\hat{\mathbf{g}}_1 = (1+u')\cos\psi + v'\sin\psi = J_o \\ \delta_v &\equiv \boldsymbol{\delta}.\hat{\mathbf{g}}_2 = -(1+u')\sin\psi + v'\cos\psi = C_{12} \end{aligned} \tag{22}$$

Hence, a comparison between equations (18) and (22) shows that $\boldsymbol{\lambda}_g \equiv [\delta_n - 1 \;\; \delta_v \;\; \psi']^T$. If the rod undergoes pure bending (Fig. 2)

$$1 + u' - \cos\psi \equiv v' - \sin\psi \equiv 0 \quad <=> \quad \delta_n \equiv \delta_v \equiv 0$$

and, therefore, $N \equiv V \equiv 0$ in agreement with our intuition.

2.4.- Constitutive Equations.

Based upon the strain measures $\boldsymbol{\lambda}_g$ defined by (18), constitutive equations for isothermal hyperelasticity are first considered. Next, the appropriate rate form of these equations is examined in order to formulate a viscoplastic constitutive model in terms of the strain measures $\boldsymbol{\lambda}_g$.

2.4.1.- Hyperelasticity

Confining our attention to isothermal processes, it is assumed that a strain energy potential $\hat{W}(X^1,\boldsymbol{\lambda}_g)$ exists such that

$$\mathbf{R}_g = \frac{\partial \hat{W}(X^1,\boldsymbol{\lambda}_g)}{\partial \boldsymbol{\lambda}_g}. \tag{23}$$

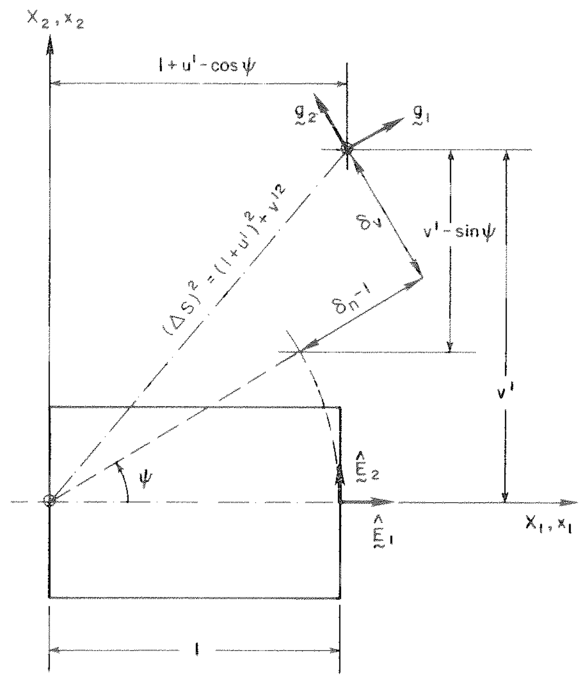

Fig. 2. Geometric interpretation of strain measures.

From this equation it follows that $G(\boldsymbol{\eta},\mathbf{w}) = \frac{d}{d\alpha}[\Pi(\mathbf{w}+\alpha\boldsymbol{\eta})]_{\alpha=0}$ where $\mathbf{w}\rightarrow\Pi(\mathbf{w})\in I\!R$ is the total potential energy function given by

$$\Pi(\mathbf{w}) = \int_0^L W(X^1,\boldsymbol{\lambda}_g)\,dX - \int_0^L q(X^1)\,v(X^1)\,dX - [\mathbf{w}.\tilde{\mathbf{R}}_x]_{\partial_R} \tag{24}$$

with $\boldsymbol{\lambda}_g$ defined in terms of $\mathbf{w}$ by Eq. (18). In the sequel, attention is restricted to the simplest model for which $\hat{W}$ is a quadratic functional in $\boldsymbol{\lambda}_g$ given by

$$\hat{W} = E\Omega(X^1)(\delta_n-1)^2 + G\Omega(X^1)\delta_v^2 + EI(X^1)(\psi')^2 \tag{25}$$

Hence, we can write

$$\mathbf{R}_g = \mathbf{D}\,\boldsymbol{\lambda}_g \tag{26}$$

where $\mathbf{D} = \mathrm{diag}\,[\,E\Omega(X^1)\quad G\Omega(X^1)\quad EI(X^1)\,]$.

2.4.2.- Rate Form

In order to formulate the viscoplastic problem it is necessary to consider the constitutive equations in rate form. Objective rates of the stress resultants and their corresponding strain measures must be obtained so that the material response may be suitably characterized. Noting the relationship between stress and strain quantities in the fixed spatial and Gaussian frames given by $\mathbf{R}_x = \mathbf{\Lambda}(\psi)\mathbf{R}_g$ and $\boldsymbol{\lambda}_x = \mathbf{\Lambda}(\psi)\boldsymbol{\lambda}_g$, respectively; the constitutive model (26) can be cast in the fixed spatial frame as

$$\mathbf{\Lambda}^T \mathbf{R}_x = \mathbf{D}\, \mathbf{\Lambda}^T \boldsymbol{\lambda}_x \tag{27}$$

Taking the time derivative of this equation one arrives at the following rate form:

$$\dot{\mathbf{R}}_x - \dot{\mathbf{\Lambda}}\, \mathbf{\Lambda}^T \mathbf{R}_x = \mathbf{\Lambda}\, \mathbf{D}\, \mathbf{\Lambda}^T \{\dot{\boldsymbol{\lambda}}_x - \dot{\mathbf{\Lambda}} \mathbf{\Lambda}^T \boldsymbol{\lambda}_x\} \tag{28}$$

It is, therefore, natural to define the rate $\overset{\square}{\mathbf{R}}$ by its components with respect to either $\{\hat{\mathbf{e}}_i\}$ or $\{\hat{\mathbf{g}}_i\}$ as

$$\overset{\square}{\mathbf{R}}_g = \left[\frac{D\mathbf{R}}{Dt}\right]_g - \mathbf{\Lambda}^T \dot{\mathbf{\Lambda}}\, \mathbf{R}_g \qquad => \qquad \overset{\square}{\mathbf{R}}_x = \dot{\mathbf{R}}_x - \dot{\mathbf{\Lambda}}\, \mathbf{\Lambda}^T \mathbf{R}_x \tag{29}$$

Constitutive equations (26) then take the rate form

$$\overset{\square}{\mathbf{R}}_g = \mathbf{D}\overset{\square}{\boldsymbol{\lambda}}_g \quad or \quad \overset{\square}{\mathbf{R}}_x = \mathbf{\Lambda D \Lambda}^T \overset{\square}{\boldsymbol{\lambda}}_x \tag{30}$$

Remarks

(i) The rate $\overset{\square}{\mathbf{R}}_g$ of the "rotated" stress resultants $\mathbf{R}_g$ admits the following interpretation. The force vector $\mathbf{R}$ can be expressed in terms of its components with respect to $\{\hat{\mathbf{g}}_i\}$ as $\mathbf{R} = R_g^\alpha \hat{\mathbf{g}}_\alpha$. Taking the material time derivative of $\mathbf{R}$ it follows that

$$\frac{D\mathbf{R}}{Dt} = \left\{\frac{D}{Dt}\left[R_g^\beta\right] + \Lambda_i^\beta\, \dot{\Lambda}_\alpha^i\, R_g^\alpha\right\}\hat{\mathbf{g}}_\beta \equiv \left[\frac{D\mathbf{R}}{Dt}\right]_g^\beta \hat{\mathbf{g}}_\beta \tag{31}$$

Hence, the components of the material time derivative of $\mathbf{R}$ with respect to $\{\hat{\mathbf{g}}_i\}$ can be expressed in matrix form as

$$\left[\frac{D\mathbf{R}}{Dt}\right]_g = \frac{D}{Dt}\left[\mathbf{R}_g\right] + \mathbf{\Lambda}^T \dot{\mathbf{\Lambda}}\, \mathbf{R}_g \tag{32}$$

A comparison of the latter with the definition of $\overset{\square}{\mathbf{R}}_g$ shows that this rate is simply the rate of change of the components of $\mathbf{R}$ with respect to $\{\hat{\mathbf{g}}_i\}$. Explicitly,

$$\overset{\square}{\mathbf{R}}_g = \frac{D}{Dt}\left[\mathbf{R}_g\right]. \tag{33}$$

(ii) The physical significance of the strain rate $\overset{\square}{\boldsymbol{\lambda}}$ may be illustrated as follows. By definition, its components with respect to $\{\hat{\mathbf{e}}_i\}$ are given by

$$\overset{\square}{\boldsymbol{\lambda}}_x = \dot{\boldsymbol{\lambda}}_x - \dot{\mathbf{\Lambda}}\, \mathbf{\Lambda}^T \boldsymbol{\lambda}_x = [v'\dot{\psi} + \dot{u}' \quad -(1+u')\dot{\psi} + \dot{v}']^T$$

Therefore, the condition $\overset{\square}{\boldsymbol{\lambda}}_x \equiv 0$ implies $\dot{u}'(1+u') + \dot{v}'v' \equiv 0$. Upon noting that the element of length ds is given by $ds^2 = ||\mathbf{F}\,\hat{\mathbf{E}}_1||^2 = (1 + u')^2 + v'^2$, one has the equivalent condition

$$\overset{\square}{\boldsymbol{\lambda}} \equiv 0 \quad <=> \quad ds^2 \equiv constant \;,\quad t \in [0,\infty)\,.$$

(iii) *(Material Frame Indifference and Invariance Under Superposed Rigid Body Motion)* Consider a superposed rigid body motion. The fixed spatial frame $\{\hat{\mathbf{e}}_i\}$ is then transformed according to to $\{\hat{\mathbf{e}}_i^+\} = \mathbf{Q}(t)\,\{\hat{\mathbf{e}}_i\}$, where $\mathbf{Q}(t)$ is any proper orthogonal tensor. Since $\mathbf{F}^+ = \mathbf{Q}(t)\,\mathbf{F}$, it easily follows that $\boldsymbol{\Lambda}^+ = \mathbf{Q}(t)\,\boldsymbol{\Lambda}$. Taking the material time derivative of this expression, making use of (29), and noting that $\mathbf{R}_x^+ = \mathbf{Q}(t)\mathbf{R}_x$, we arrive at the following transformation rules

$$\overset{\square}{\mathbf{R}}{}_x^+ = \mathbf{Q}(t)\,\overset{\square}{\mathbf{R}}_x \qquad \overset{\square}{\mathbf{R}}{}_g^+ = \overset{\square}{\mathbf{R}}_g \tag{34}$$

While the rate $\overset{\square}{\mathbf{R}}_x$ is objective, the rate $\overset{\square}{\mathbf{R}}_g$ of the rotated stress has the stronger property of being invariant under superposed rigid body motion. The desirability of this property was pointed out by [12].

2.4.3.- Viscoplasticity.

We postulate an additive decomposition of the total strain rate $\overset{\square}{\boldsymbol{\lambda}}_g$ into elastic and viscoplastic parts: $\overset{\square}{\boldsymbol{\lambda}}_g = \overset{\square}{\boldsymbol{\lambda}}{}_g^e + \overset{\square}{\boldsymbol{\lambda}}{}_g^{vp}$, where the elastic part $\overset{\square}{\boldsymbol{\lambda}}{}_g^e$ is related to $\overset{\square}{\mathbf{R}}_g$ by Eq. (30). Furthermore, we assume that the evolution of the viscoplastic part $\overset{\square}{\boldsymbol{\lambda}}{}_g^{vp}$ is given by the rate equation

$$\overset{\square}{\boldsymbol{\lambda}}{}_g^{vp} = \frac{1}{\tau} < f(\mathbf{R}_g) > \frac{\partial f}{\partial \mathbf{R}_g} \equiv \frac{1}{\tau}\,\boldsymbol{\beta}(\mathbf{R}_g) \tag{35}$$

where $f(\mathbf{R}_g)$ is the plastic flow potential in stress resultant space, τ is the relaxation time of the viscous process, and $< x > = \tfrac{1}{2}(x + |x|)$ is the Macauley bracket. The proposed viscoplastic constitutive model is then defined by the rate equation

$$\overset{\square}{\boldsymbol{\lambda}}_g = \mathbf{D}^{-1}\overset{\square}{\mathbf{R}}_g + \frac{1}{\tau}\,\boldsymbol{\beta}(\mathbf{R}_g) \tag{36}$$

Equations (17) and (36) completely describe the evolution of the system provided f is known.

The Plastic Flow Potential. The formulation of the viscoplastic model in terms of stress resultants relies upon the postulated existence of the flow potential $f(N, V, M)$. The problems associated with obtaining f have been discussed in the literature [13,14], and hence will not be treated in detail here. However, some comments regarding assumptions surrounding the plastic flow potential are in order:

(i) The form of $f(N, V, M)$ depends upon the geometry of the cross section; not merely the local constitution of the material. The projections $f(N, V, 0)$ and $f(N, 0, M)$ are easily obtained but the case of V and M both nonzero presents considerable difficulty. In fact, the projection $f(0, V, M)$ has been obtained only in a few cases. The usual approach to the problem of estimating f is to employ the bounding theorems of plasticity.

(ii) It is known that for certain cross sectional geometries, most notably the I-section, f is not everywhere convex [15,16]. Since plasticity theories generally depend upon convexity of the flow potential, some objection to the stress resultant approach might be raised. It should be noted, however, that the regions of non-convexity seem to be confined to combinations of (N, V, M) not possibly attained by beams in reasonable problems (ie. problems in which the length exceeds half the depth of the section).

For the purpose of illustration attention will be confined to rectangular cross sections. The projections $f(N,0,M)$, $f(0, V, M)$, and $f(N, V, 0)$ have been estimated for this case [13,14]. Denoting by $m = M/M_o$, $v = V/V_o$, and $n = N/N_o$, where $(\ )_o$ indicates the fully plastic value in the absence of the other two stress resultants, we have the following projections:

$$
\begin{aligned}
f(n, v, 0) &= n^2 + v^2 - 1 \\
f(n, 0, m) &= |m| + n^2 - 1 \\
f(0, v, m) &= |m| + v^4 - 1.
\end{aligned}
\tag{37}
$$

The potential generating these projections is, of course, not unique. However, the following plausible potential is suggested:

$$
f(n, v, m) = |m| + n^2(1 + v^2) + v^4 - 1. \tag{38}
$$

The surface $f=0$ and the rigorous lower bound obtained by Neal [14] are shown in Fig. 3 along with the potential

$$
\bar{f}(n, v, m) = (1 - n^2)(|m| + n^2 - 1) + v^4 \tag{39}
$$

which was suggested by Neal [14]. Clearly, f is in better correspondence with the lower bound solution than is $\bar{f}$. However, since an upper bound solution does not exist, it is difficult to assess the advantage of either one.

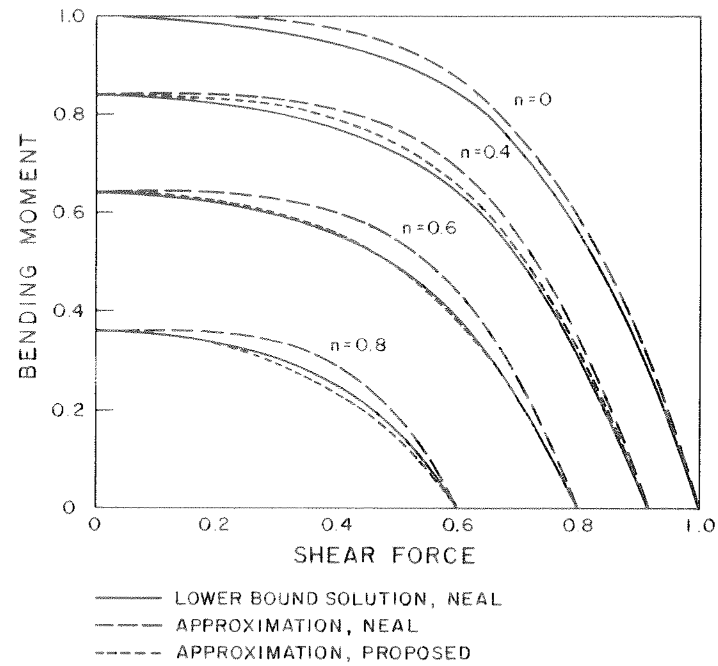

Fig. 3. Moment-Shear-Axial force interaction diagram, rectangular section.

2.5.- Solution Procedure. Linearization .

The linearization of the weak form of the equilibrium equations about a intermediate configuration plays a key role in numerical implementations employing an iterative solution procedure. A complete account of linearization procedures in the general context of infinite dimensional manifolds can be found in [9].

Consider an intermediate configuration $\overline{\mathbf{w}} : \mathbb{R} \rightarrow \mathbb{R}^3$. Let $\Delta\mathbf{w} : \mathbb{R} \rightarrow \mathbb{R}^3$ be a superposed infinitesimal deformation; that is, a vector field covering $\overline{\mathbf{w}}(X^1)$. The linear part of $G(\boldsymbol{\eta},\mathbf{w})$ at $\overline{\mathbf{w}}(X^1)$ will be denoted by $L[G]_{\overline{\mathbf{w}}}$. Introducing the notation

$$\mathbf{A}_G = \begin{bmatrix} \mathbf{O} & \dfrac{d\boldsymbol{\Lambda}}{d\psi}(\overline{\psi}).\overline{\mathbf{R}}_g \\ \overline{\mathbf{R}}_g^T.\dfrac{d\boldsymbol{\Lambda}^T}{d\psi}(\overline{\psi}) & \mathbb{F}^T(\overline{\mathbf{w}}).\dfrac{d^2\boldsymbol{\Lambda}}{d\psi^2}(\overline{\psi}).\overline{\mathbf{R}}_g \end{bmatrix}; \qquad \boldsymbol{\Xi}(\overline{\mathbf{w}}) = \begin{bmatrix} \boldsymbol{\Lambda}(\overline{\psi}) \\ \mathbb{F}^T(\overline{\mathbf{w}}).\dfrac{d\boldsymbol{\Lambda}}{d\psi}(\overline{\psi}) \end{bmatrix}^T \tag{40}$$

and defining the linear operator $\mathbb{B} : [H^1(0,L)]^3 \rightarrow [L^2(0,L)]^4$ by

$$\mathbf{w} \rightarrow \mathbb{B}(\mathbf{w}) \equiv [\ \mathbb{F}^T(\mathbf{w}) \quad \psi\ ]^T \tag{41a}$$

the linearized weak form of the equilibrium equations may be conveniently written in matrix notation as

$$L[G]_{\overline{\mathbf{w}}} = \int_0^L \mathbb{B}^T(\boldsymbol{\eta})\ \mathbf{A}_G(\overline{\mathbf{R}}_g,\overline{\mathbf{w}})\ \mathbb{B}(\Delta\mathbf{w})\ dX$$

$$+\int_0^L \mathbb{B}^T(\eta)\ \Xi^T(\bar{\mathbf{w}})\ D\mathbf{R}_g(\bar{\mathbf{w}}).\Delta\mathbf{w}\ dX\ +\ G(\eta,\bar{\mathbf{w}}) \tag{41}$$

The first two terms in (41) give rise to the tangent stiffness at the configuration $\bar{\mathbf{w}}(X^1)$, the first term being the geometric part. The last term, representing the residual or out-of-balance force at the configuration $\bar{\mathbf{w}}(X^1)$, has the explicit expression

$$-\ G(\eta,\bar{\mathbf{w}}) = [\eta.\bar{\mathbf{R}}_X]_{\partial_R} - \int_0^L \mathbb{B}^T(\eta)\ \Xi^T(\bar{\mathbf{w}})\ \bar{\mathbf{R}}_g\ dX \tag{42}$$

and vanishes identically if $\bar{\mathbf{w}}(X^1)$ is an equilibrium configuration. By setting $L[G]_{\bar{\mathbf{w}}} = 0$ for any $\eta \in W$ in (41) and introducing the expressions for $\bar{\mathbf{R}}_g$ and the Frechet differential $D\mathbf{R}_g(\bar{\mathbf{w}}).\Delta\mathbf{w}$, one obtains a classical variational problem from which the incremental deformation $\Delta\mathbf{w} : \mathbb{R} \to \mathbb{R}^3$, such that $\Delta\mathbf{w}(X^1) + \bar{\mathbf{w}}(X^1) \in W$, may be obtained.

Hyperelasticity. From the constitutive equation (26) it follows that

$$D\mathbf{R}_g(\bar{\mathbf{w}}).\Delta\mathbf{w} = \mathbf{D}\ \Xi(\bar{\mathbf{w}})\mathbb{B}(\Delta\mathbf{w}) \tag{43}$$

and $\mathbf{R}_g$ is given directly by (26) in terms of $\boldsymbol{\lambda}_g$.

Viscoplasticity. Due to the time dependence of the viscoplastic problem, the solution procedure first involves the time integration of the constitutive equations (36). For each discrete interval $[t_o,\ t_o{+}\Delta t]$, the last term in equation (36) is integrated numerically by setting [7]

$$\frac{1}{\tau}\int_{t_o}^{t} \beta(\mathbf{R}_{g_\xi})\ d\xi = \frac{\Delta t}{\tau}\beta(\mathbf{R}_{g_\alpha}) \tag{44}$$

where we have used the notation

$$\mathbf{R}_{g_\alpha} = (1-\alpha)\mathbf{R}_{g_o} + \alpha\mathbf{R}_{g_t} \qquad 0 \leqslant \alpha \leqslant 1 \tag{45}$$

The subscripts "o" and "t" refer to values of functions at t_o and $t = t_o{+}\Delta t$, respectively. Substitution of (44) into (36), noting the simple form of the expression for the rate, leads to

$$\Psi_t \equiv -(\boldsymbol{\lambda}_{g_t} - \boldsymbol{\lambda}_{g_o}) + \mathbf{D}^{-1}\ (\mathbf{R}_{g_t} - \mathbf{R}_{g_o}) + \frac{\Delta t}{\tau}\ \beta(\mathbf{R}_{g_\alpha}) = 0 \tag{46}$$

From this equation it immediately follows that the term $D\mathbf{R}_g(\bar{\mathbf{w}}).\Delta\mathbf{w}$ appearing in the weak form (41) is given at any configuration $\bar{\mathbf{w}}(X^1)$ by

$$D\mathbf{R}_g(\bar{\mathbf{w}}).\Delta\mathbf{w} = [\mathbf{D}^{-1} + \alpha\frac{\Delta t}{\tau}\beta'(\mathbf{R}_{g_\alpha})]^{-1}\ \Xi(\bar{\mathbf{w}})\ \mathbb{B}(\Delta\mathbf{w})\ \equiv\ \boldsymbol{\Omega}_t\ \Xi(\bar{\mathbf{w}})\ \mathbb{B}(\Delta\mathbf{w}) \tag{47}$$

In view of (36) and (40) it is clear that knowledge of the value $\overline{\mathbf{R}}_{g_t}$ at $\overline{\mathbf{w}}(X^1)$ completely determines the linearized weak form (41) of the equilibrium equations. Hence, its solution $\Delta\mathbf{w}$ defines the subsequent configuration $\mathbf{w}(X^1) = \overline{\mathbf{w}}(X^1) + \Delta\mathbf{w}(X^1)$. From a numerical point of view, the only difference between the elastic and the viscoplastic model under consideration is that the later requires the solution the non-linear equation (46) to obtain $\mathbf{R}_{g_t}$ given $\boldsymbol{\lambda}_{g_t}$ whereas in the former $\mathbf{R}_g$ is directly given by $\mathbf{R}_g = \dfrac{\partial \hat{W}(X^1, \boldsymbol{\lambda}_g)}{\partial \boldsymbol{\lambda}_g}$.

Hughes and Taylor [7] have proposed estimating $\overline{\mathbf{R}}_g$ by its linear part. Such a procedure can be viewed as a simultaneous *global* iteration on the linearized momentum balance and constitutive equations. This approach gives rise to the constitutive residual Ψ_t, defined by (46), which must vanish when the solution is achieved.

The procedure advocated by [7] is modified here, on the other hand, to employ *global* iteration only on the linearized weak form of equilibrium equations, with "exact" satisfaction of the non-linear constitutive equation (46) at each intermediate configuration. "Exact" satisfaction of the constitutive equation is achieved by *local* iteration on its linearization with respect to the stress. Our motivation for this procedure is that in a finite element *displacement* model, the only independent variables are the incremental displacements. The constitutive equations are regarded as a set of constraints which must be satisfied point-wise when the weak form of momentum balance is solved by an iterative procedure. From a computational point of view, the procedure proposed here results in a considerable savings in the required storage and leads to a reduction in the total number of global iterations required to achieve convergence.

The numerical treatment of the weak form (41) by a finite element technique involves the spatial discretization of the open interval $(0, L)$, and the interpolation of $\boldsymbol{\eta} \in W$ and $\Delta\mathbf{w}$ by means of shape functions. Since $\boldsymbol{\eta}$ lies in $H^1(0, L)$, C^0 shape functions are sufficient [18]. Following standard procedures [17,18], the final result may be expressed as

$$\mathbf{K}_t \, \Delta\mathbf{W}_t = \mathbf{f}_t \tag{48}$$

where $\mathbf{K}_t$ is the global tangent stiffness, $\Delta\mathbf{W}_t$ is the vector of incremental nodal displacements, and $\mathbf{f}_t$ is the residual force vector at the current configuration. $\mathbf{K}_t$ and $\mathbf{f}_t$ are given by

$$\mathbf{K}_t = \sum_e \int_0^L \mathbf{B}_t^{e^T} \, [\mathbf{A}_{G_t}{}^e + \boldsymbol{\Xi}_t^{eT} \, \boldsymbol{\Omega}_t^e \, \boldsymbol{\Xi}_t^e] \, \mathbf{B}_t^e \, dX$$

$$\mathbf{f}_t = \mathbf{F}_t - \sum_e \int_0^L \mathbf{B}_t^{e^T} \, \boldsymbol{\Xi}_t^{eT} \, \overline{\mathbf{R}}_{g_t}{}^e \, dX \tag{49}$$

where $\mathbf{F}_t$ is the vector of specified nodal forces, and $\mathbf{B}_t^e$ is given in term of the shape functions in the obvious manner. The proposed algorithm is summarized in Table 1. The superscripts "e" refer to nodal values of the variables within a typical element e.

TABLE 1.

Algorithm for Elasto-Viscoplasticity

Initiate Solution at $t = t_o$
For Each $t = t_o + n\Delta t$, while $\|\|\mathbf{f}_t\|\| > tol$
Form $\mathbf{K}_t$ and $\mathbf{f}_t$
Solve $\mathbf{K}_t \, \Delta\mathbf{W}_t = \mathbf{f}_t$
Update $\mathbf{W}_t \leftarrow \mathbf{W}_t + \Delta\mathbf{W}_t$
For Each Element e, while $\|\|\mathbf{\Psi}_t^e\|\| > tol$
Compute $\boldsymbol{\lambda}_{g_t}^e$, $\mathbf{\Psi}_t^e$, and $\mathbf{\Omega}_t^e$
Update $\mathbf{R}_{g_t}^e \leftarrow \mathbf{R}_{g_t}^e - \mathbf{\Omega}_t^e . \mathbf{\Psi}_t^e$

3.- STRESS COMPONENT FORMULATION

In this section, we consider the elasto-viscoplastic problem in a three dimensional setting. The weak statement of the equilibrium equations (10) together with the local form of the constitutive equations, comprise the field equations suitable for a numerical treatment by the finite element method. Since the development of these equations is well known [9], we restrict our presentation to an outline of the relevant results.

3.1.- Weak Form of Momentum Balance. Constitutive Equations.

Following standard procedures [9] the weak form of the non-linear equilibrium equations (10) may be expressed as

$$G(\boldsymbol{\eta}, \mathbf{x}) \equiv \int_B \mathbf{P}{:}GRAD\ \boldsymbol{\eta} dV - \int_B \rho_{ref} \mathbf{B}.\boldsymbol{\eta} dV - \int_{\partial B_t} \bar{\mathbf{t}}.\boldsymbol{\eta} dS = 0 \tag{50}$$

for any kinematically admissible variation $\boldsymbol{\eta}$ satisfying homogeneous conditions on the part of the boundary ∂B_u where the deformation map is prescribed. For the problem at hand

$B = (0, L) \times \Omega$ and $\partial B_t = \partial_t \bigcup \partial \Omega$, where ∂_t is that part of the boundary where tractions are prescribed.

Isothermal hyperelasticity. The constitutive equations may be expressed in terms of the second Piola-Kirchhoff stress tensor $\mathbf{S}(\mathbf{X},\mathbf{E}) = \mathbf{F}(\mathbf{X})\mathbf{P}(\mathbf{X},\mathbf{F})$ as : $\mathbf{S} = \rho_{ref} \frac{\partial \overline{W}(\mathbf{X},\mathbf{E})}{\partial \mathbf{E}}$, where $\overline{W}(\mathbf{X},\mathbf{E})$ is the strain energy potential expressed in terms of the Lagrangean strain tensor $\mathbf{E} = \frac{1}{2}(\mathbf{C} - \mathbf{1})$. We restrict our attention to a rate form of this constitutive equation expressed as

$$\dot{\mathbf{S}}(\mathbf{E}) = \mathbf{D}(\mathbf{E}).\dot{\mathbf{E}} \tag{51}$$

where $\mathbf{D} = D^{IJKL}\{\hat{\mathbf{E}}_I \otimes \hat{\mathbf{E}}_J \otimes \hat{\mathbf{E}}_K \otimes \hat{\mathbf{E}}_L\}$ is a forth-order material tensor.

Viscoplasticity. The formulation of the viscoplastic model is accomplished by postulating an additive decomposition of the Lagrangean strain rate into elastic an viscoplastic parts: $\dot{\mathbf{E}} = \dot{\mathbf{E}}^e + \dot{\mathbf{E}}^{vp}$. Such a decomposition may be justified on thermodynamic grounds [19, references therein]. The elastic part is given by (51) and the evolution of the viscoplastic part is assumed to be given by the rate equation [8]

$$\dot{\mathbf{E}}^{vp} = \frac{1}{\tau} < F(\mathbf{S}) > \frac{\partial f}{\partial \mathbf{S}} \equiv \frac{1}{\tau}\boldsymbol{\beta}(\mathbf{S}) \tag{52}$$

where $f(\mathbf{S})$ is the viscoplastic flow potential expressed in terms of $\mathbf{S}$. The rate equation (52) is formally correct, simple, and clearly motivated by the "infinitesimal" theory [20]. The validity of (52) may be physically questionable in the range of truly large deformations, and hence we restrict its use to second order problems. Inasmuch as (52) reduces to the appropriate rate for an isotropic material in the linearized theory, it appears to be reasonable for second order problems. The function $F(\mathbf{S})$ and the relaxation time τ, reflect the viscous properties of the particular material. Suitable choices for well known materials have been discussed in the literature [20]. For simplicity, a Von-Mises type of potential $f \equiv \frac{3}{2}[\mathbf{S}{:}\mathbf{S} - \frac{1}{3}\mathrm{tr}^2(\mathbf{S})] - k^2$ will be assumed. Inclusion of isotropic or kinematic hardening may be accomplished by introducing internal variables [20]. Rate independent plasticity can be obtained from model (52) as the inviscid limit when the relaxation time $\tau \to 0$. Such a limiting process may be viewed a the enforcement of the consistency condition by a penalty procedure. The function $F(\mathbf{S})$ then needs to satisfy the condition $\lim_{\tau \to 0} \frac{1}{\tau} < F(\mathbf{S}) > = \lambda$, where λ is indeterminate. A rigorous treatment of this limiting process can be found in [21]. Here, the choice $F = \frac{f}{k^2}$ will be adopted. The viscoplastic constitutive model is then expressed in rate form as

$$\dot{\mathbf{E}} = \mathbf{D}^{-1}\dot{\mathbf{S}} + \frac{1}{\tau}\boldsymbol{\beta}(\mathbf{S}). \tag{53}$$

3.2.- General Solution Procedure.

Formally, the solution procedure is equivalent to that discussed in the previous section. The linearization of the weak form of momentum balance (50) about an intermediate configuration $\bar{\phi} : B \rightarrow \mathbb{R}^3$ leads to the expression [9]

$$L[G]_{\bar{\phi}} \equiv \int_B GRAD\ \eta.(\bar{S}\otimes 1 + \bar{F}^T \left[\frac{\partial S}{\partial E} \right]_{\bar{\phi}} \bar{F})GRAD\ (\Delta\phi)dV + G(\eta, \bar{x}) \tag{54}$$

where a superposed "‾" designates the corresponding variable evaluated at the configuration $\bar{x} = \bar{\phi}(X)$, and $\Delta\phi : B \rightarrow \mathbb{R}^3$ the incremental motion, a vector field covering $\bar{\phi} : B \rightarrow \mathbb{R}^3$.

Hyperelasticity. Equation (54) together with the constitutive equation $S = \rho_{ref} \dfrac{\partial \overline{W}(E)}{\partial E}$ leads, in the static case, to a classical variational problem which can be treated by standard finite element techniques [17,18].

Viscoplastic model. The solution of the viscoplastic problem requires first the time integration of the constitutive model (53) over an incremental time step $[t_0,\ t_0+\Delta t]$. Following [7], the result may be written as

$$\Psi_t = -(E_t + E_o) + D^{-1}(S_t - S_o) + \frac{\Delta t}{\tau}\beta(S_\alpha) = 0 \tag{55}$$

where we have again set

$$S_\alpha = (1-\alpha)\ S_o + \alpha\ S_t \qquad 0 \leqslant \alpha \leqslant 1 \tag{56}$$

Hence, for the viscoplastic constitutive model one obtains

$$\frac{\partial S}{\partial E} = [D^{-1} + \alpha \frac{\Delta t}{\tau}\ \beta'(S_\alpha)]^{-1} \tag{57}$$

and a solution procedure similar to that outlined in Table 1, with the obvious changes in notation, may be employed.

By introducing the kinematics expressed in Eq. (6), one considerably simplifies the task of solving the three dimensional formulation discussed so far. In this way, one essentially treats a one dimensional problem (ie. the kinematic variables depend only upon X^1) without completely giving up the ability to discern local phenomena, such as propagation of yielding throughout a cross section. Solution of specific problems using this approach generally can only be carried out by employing numerical integration over the cross sectional domain, as outlined in the following section.

3.3.- Numerical Integration over the Cross Section.

Making use of the method of successive approximations, it is possible to show that only linear strain measures are explicitly involved in the second order approximation to the equilibrium equations (10) [4]. Consequently, the linearized kinematics given by (6), which are capable of accounting for the effect of transverse warping due to shear deformation and the Poisson's effect, can be used to develop a second order approximate solution. If this approach is followed, the deformation gradient $\mathbf{F}(\mathbf{X})$ appearing in the linearized weak form (54) is then expressed in terms of the set of kinematic variables $\{\bar{u},\ \bar{v},\ \bar{\psi},\ \bar{\beta}\}$.

For analytical purposes, it is advantageous to regard the kinematic variable $\bar{\beta}(X^1)$ as a dependent variable through the relationship $\bar{\beta} = \bar{v}' - \bar{\psi}$. From a numerical standpoint, however, it is convenient to maintain the simple structure of a C^0 interpolation, which can be achieved if $\bar{\beta}$ is regarded as an independent variable. In the context of Kantorovich's projection method [11], both situations are admissible (although not exactly equivalent [11]), the difference being that in the former, stress boundary conditions on $\partial\Omega$ are enforced at the outset. Regarding $\bar{\beta}(X^1)$ as independent, and assuming that $\nu\bar{u}' \approx 0^{\dagger}$, the deformation gradient can be interpolated over a typical element e as

$$\mathbf{F}^e(\mathbf{X}) = \mathbf{1} + \sum_{\alpha=1}^{Nodes} \mathbf{B}_\alpha^e(\mathbf{X})\ \mathbf{U}^\alpha \tag{58}$$

where the displacement variables $\mathbf{u}(X^1) \equiv [\ \bar{u}\quad \bar{v}\quad \bar{\psi}\quad \bar{\beta}\ ]^T$ are interpolated from the nodal displacements $\mathbf{U} \equiv [\ U\quad V\quad \Psi\quad B\ ]^T$ as

$$\mathbf{u}(X^1) = \sum_{\alpha=1}^{Nodes} h_\alpha(X^1)\ \mathbf{U}^\alpha \tag{59}$$

and the matrix $\mathbf{B}_\alpha^e(\mathbf{X})$ is a third order tensor defined by

† This approximation is only required to maintain the C^0 interpolation structure. It is not essential to the numerical formulation.

$$
\mathbf{B}_\alpha^e(\mathbf{X}) = \left\| \begin{array}{cccc}
h'_\alpha & 0 & -X^2 h'_\alpha & -\kappa\Phi_1 h'_\alpha \\
0 & h'_\alpha & 0 & -\nu\dfrac{\kappa G\Omega}{EI}\Phi_2 h_\alpha \\
0 & 0 & 0 & -\nu\dfrac{\kappa G\Omega}{EI}\Phi_3 h_\alpha \\
\hline
0 & 0 & -h_\alpha & -\kappa\Phi_{1,2} h_\alpha \\
0 & 0 & \nu\Phi_{2,2} h'_\alpha & 0 \\
0 & 0 & \nu\Phi_{3,2} h'_\alpha & 0 \\
\hline
0 & 0 & 0 & -\kappa\Phi_{1,3} h_\alpha \\
0 & 0 & \nu\Phi_{2,3} h'_\alpha & 0 \\
0 & 0 & \nu\Phi_{3,3} h'_\alpha & 0
\end{array} \right\|
$$

Note that each submatrix of $\mathbf{B}_\alpha^e$ corresponds to a column of the matrix $\mathbf{F}^e$, and that the notation $\Phi_{i,j} \equiv \dfrac{\partial\Phi_i}{\partial X^j}$ has been used. Knowing the expression for the matrix $\mathbf{B}^e$, the tangent stiffness and right-hand-side can be computed as in Eq. (49), with the appropriate reinterpretation of notation.

4.- NUMERICAL EXAMPLES

In this section numerical examples are presented which have been selected to emphasize the important features of the preceding formulations. The five "elements" employed in the numerical computation were implemented in the general purpose finite element program FEAP, described in Chapter 24 of [17]. Two of the elements were devoted to the stress resultant formulations presented in Section 2; one reflecting fully nonlinear kinematics with the plane sections hypothesis and the other second order approximate kinematics allowing for the effect of warping. The other three elements reflect the stress component formulation of Section 3. Two of these utilize the kinematic hypothesis expressed by equation (6) and employ numerical integration over the cross section of the beam. One of these elements is specifically for the case of a rectangular cross section, and the other is for an I-beam. The last element is a finite deformation, 2-d (plane stress/strain), elastic element developed in [22]. All beam elements were implemented with the possibility of 2-node or 3-node interpolation. Reduced integration along X_1 was employed to prevent "shear locking" [22]. Computations were done on a VAX 11/780 computer.

The first three examples are well known problems of large displacement of elastic beam structures: Euler's elastica, pure bending of an Euler beam, and the buckling of a fixed-hinged circular arch under a point load at its crown. Each of these problems was solved using a stress resultant beam element reflecting the plane sections hypothesis expressed by Eq. (4). The purpose of presenting these examples is to show the good accuracy and convergence properties of the large displacement formulation. Example 4, the elasto-plastic snap-through of a three-hinged arch, involves finite rotations and strains and thereby illustrates the properties of the rates of rotated stresses and strains discussed in section 2.4.2. It should be noted that, inasmuch as the formulation is in terms of stress resultants, the computational costs involved are minimal.

1.- Euler's Elastica. The first example is a cantilever subjected to a compressive end thrust, the so called Euler's elastica. The classical problem of Euler addresses the idealized situation wherein the line of centroids is assumed to be perfectly inextensible and no shear deformation is allowed to occur. Accordingly, in view of (22), $ds_o^2 = (1 + u')^2 + v'^2 \equiv 1$, and $\delta_v \equiv C_{12} \equiv 0$. These constraints can be enforced by a penalty procedure, simply by regarding $G\Omega$ and $E\Omega$ in (25) as penalty parameters, and requiring that both $G\Omega/EI \rightarrow \infty$ and $E\Omega/EI \rightarrow \infty$. From a numerical stand point, this procedure amounts to specifying values for $G\Omega$ and $E\Omega$ to be suitably larger than the bending stiffness EI. For general nonlinear elastostatics, care must be exercised in applying the penalty procedure [23]. The post buckling behavior of the column is shown in Fig. 4.

2.- Pure Bending of an Euler Beam. The second example is an Euler beam fixed at one end and subjected to an applied end moment at the other. As the bending moment increases the radius of curvature of the deformed beam decreases, the net effect being that the beam "curls up". The exact solution to this problem is, of course, $\rho = \frac{M}{EI}$. Ten quadratic elements were used to obtain the solutions shown in Fig. 5. However, exact values of end displacement and rotation were also obtained with a single element. The solution at each load step was obtained (in both cases) in two iterations.

3.- Buckling of a Fixed-Hinged Circular Arch. The buckling and post-buckling behavior of a circular arch, fixed at one end, hinged at the other, and subjected to a point load applied at the crown is shown in Fig. 6. The solution was obtained using 20 quadratic elements. The good correspondence between the finite element solution and the exact solution obtained by DaDeppo and Schimdt [24] can be seen in the figure. The deformed arch at various stages of loading is also shown in Fig. 6.

Other finite element solutions of this problem have been obtained by Wood and Zienkiewicz [loc. cit. 17] and by Pinsky and Taylor [8]. Wood and Zienkiewicz solve the problem using a two dimensional Lagrangian approach. Pinsky and Taylor, on the other hand, employ a stress component formulation , similar to that presented in Section 3, in conjunction with the plane sections kinematics expressed by equation (6) and numerical integration over the cross section. Both [17] and [8] report a value of the buckling load of 925, comparing with the exact solution given by DaDeppo and Schmidt of 897, and the value of 906 obtained herein. Pinsky and Taylor do not report values in the post buckling range.

4.- Snap-through of a Three Hinged Arch. The fourth example treated is the elastic and elasto-plastic snap-through of a three-hinged arch point loaded at its apex. The elasto-plastic problem involves, in addition to the massive geometric non-linearities and instability phenomenon of the elastic problem , rate independent elasto-plastic material response. These problems are, however, simple enough to allow exact solutions in both cases, which are used here to assess the performance of the rates of rotated stress and strain, $\overset{\square}{\mathbf{R}}_g$ and $\overset{\square}{\lambda}_g$ discussed in section 2.4.2.

As shown in Fig. 7, the exact and computed solution (obtained with a single linear element) are in agreement, confirming the observations of section 2.4.2. Note that the elastic unloading at snap-through has been precisely captured in the computed solution of the elastic-plastic problem.

5.- Buckling of a Beam Flexible in Shear. In this example we consider the loss of stiffness and eventual buckling of a column extremely flexible in shear. The multilayer elastomeric bearing (transversally isotropic column) [22,26,27,28] and the sandwich beam [25] with soft core furnish two examples of practical interest in which this situation is typically found. Expressions for the buckling load for both types of columns based on elementary beam theory were derived by Haringx [26] and Plantema † [25] for the bearing and the sandwich respectively, and have been found to correspond well with experimental results [25,26,27,28]. A more refined expression for the transversally isotropic column was recently proposed by Simo [3,4].

The results plotted as diamonds ( ) on curve 1, Fig. 8, were obtained with a stress resultant formulation employing the kinematic assumption (4). It is clear that the results are in complete agreement with the analytical solution of Haringx. The results represented as squares (□) on curve 2, Fig. 8, were obtained with a stress resultant formulation employing the kinematic assumption (6), which includes the effect of transverse warping. These results, which are in complete agreement with the solution obtained by Simo [3,4] for a transversally homogeneous beam, illustrate the important influence of the effect of warping on the buckling of a beam [3,4]

†The same expression was initially proposed by Timoshenko [29] for a homogeneous beam.

The results plotted on curve 3, Fig.8, were obtained using the three dimensional constitutive model

$$E_{ij} = \frac{1+\nu}{E} S_{ij} - \frac{\nu}{E} tr(\mathbf{S})\delta_{ij} \quad (i=j), \qquad E_{ij} = \frac{1}{2G} S_{ij} \quad (i \neq j) \tag{61}$$

where $E^{\#}$, $\nu^{\#}$, and $G^{\#}$ are independent elastic constants. The results represented by circles (O) were obtained using the stress component formulation with the kinematic assumption (6), and those represented by triangles (Δ) were obtained with a two dimensional finite deformation element reported in [22]. The correspondence between the two elements is seen to be excellent, attesting to the accuracy of the numerical integration over the cross section procedure when the kinematics (6) are employed. These results display a remakable feature of the constitutive model (61). *Both computed solutions agree completely with the analytical expression for the response and buckling load of the sandwich beam.* Clearly, (61) leads to a gross underestimate of the stiffness and buckling load of a (transversally) homogeneous column with low shear modulus.

An explanation of the previous observation was given in [4] where an approximate correction was also proposed. If G is taken to be the shear modulus of the linear theory, then the value of $G^{\#}$ appearing in (61) is approximately given by $G^{\#} = G + P/\Omega$ in the presence of axial load P. $E^{\#}$ and $\nu^{\#}$ are reasonably estimated by their counterparts in the linear theory. The circles (O) plotted on curve 2, Fig. 8, were obtain using this correction. The agreement with previous results should be noted.

We now turn our attention to problems involving high shear and material inelasticity. In each of the examples presented, rate independent plasticity is obtained by a penalty approach from the viscoplastic model by letting $\tau \to 0$, as mentioned in Section 3.1. Numerically, the penalty is enforced by specifying suitably small values of the relaxation time τ. It was found in these examples that, in order to keep the values of $F(\mathbf{S})$ and $f(\mathbf{R}_g)$ less than $\approx 10^{-4}$, the values of τ were on the order of 10^0 and 10^{-5}, respectively. The maximum number of local iterations required to reduce the norm of the constitutive residual to less than 10^{-12} was generally around 10 in these examples. An improvement in convergence rate of these local iterations was accomplished by saving the converged value from the previous global iteration and using it as a starting value in the following one. Hence, as the global iterations converge, fewer local iterations are required (usually only one near a converged solution).

6.- Collapse of a Fixed-Fixed Beam. We consider a beam fixed at both ends, point loaded at $3L/4$. The dimensions of the beam are such that the smaller span has a length equal to its depth. A nonuniform mesh of 13 quadratic elements was employed in the solution, the smaller elements being located at the supports and at the point of load.

The purpose of the example is to contrast the stress resultant and stress component approaches. As was previously mentioned, the stress resultant approach requires postulating a yield potential in terms of the stress resultants, the stress component formulation mitigates this problem, but at a substantial increase in computing cost.

The response of the beam to the imposed loading is shown in Fig. 9 for both stress resultants and stress components. The multi-linear character of the solution for the stress resultants resembles the classical elasto-plastic collapse of such a beam. The present solution, however, reflects the influence of shear both on the deformations and the value of the collapse load. A simple collapse analysis neglecting moment-shear interaction leads to a value of the collapse load of 27, compared with the values of 21.8 for the stress resultant element accounting for this effect. The stress component formulation, employing numerical integration over the cross section of the beam, gives a smoother solution reflecting propagation of yielding throughout the cross section, and exhibiting a collapse load of 23.5. The state of yielding for this structure at various stages of loading is also shown in Fig. 9. The evolution of the shape of the elastic-plastic interface is of considerable interest. Initial yielding occurs at the extreme fibers at one support and under the load. The pattern of yielding at collapse clearly shows that the cause of collapse is a shear mechanism. A lower value of the collapse load for the stress resultant approach is expected since the yield potential is based on a lower bound solution to the interaction problem.

7.- Cyclically Loaded Shear Beam. An effect captured by the stress component formulation that is ignored by a stress resultant approach is that of residual stress distributions over a cross section. An example exhibiting this effect is a cantilever beam cyclically loaded with a tip shear. The results of this example are shown in Fig. 10. One can see the increased roundedness of the force deflection curve that occurs upon load reversal due to the residual stresses locked in from the previous inelastic excursion. The stress resultant element would, of course, give a bilinear, perfectly plastic response and hence is not shown. It is worthy of note however that the collapse load for the stress resultant model, which can be found directly from equation (38) with $N = 0$ and $M = VL$, is 121.1, compared with 120.0 for the stress component model. The correspondence between the two collapse loads is better in this case than the previous example due, perhaps, to the fact that the relationship (38) was derived specifically for the cantilever problem but only plausibly extended to more general situations [13,14].

8.- Cyclically Loaded I-Beam. This example points out another important advantage of the stress component formulation utilizing numerical integration over the cross section: The analysis of beams having cross sections of complicated shape. When it is possible to obtain the appropriate coordinate functions $\Phi_I(X^2, X^3)$, one can easily account for the two dimensional nature of the cross section geometry. A method for computing Φ_1 has been proposed in [6] for cross sections, such as the I-section, which can be idealized as "thin walled" or locally one dimensional. This approach is especially appealing for cross sectional shapes for which the yield potential in terms of stress resultants is not known or else not easily expressed.

The response of a short, fixed-fixed I-beam is shown in Fig. 11. Also shown in the figure is the propagation of yielding in the web region (note that the flanges never yield) during the virgin monotonic excursion. The extent of yielding when the beam is in a regime of unconstrained plastic flow is especially interesting. The distribution of the stress components S_{11} and S_{12} have also been plotted in the figure. The distribution of stress at full plastic flow lends credence to some of the commonly used approximations for determining the collapse load of a beam under high shear.

5.- CLOSURE

The finite deformation, elasto-viscoplastic response of beams has been considered from a numerical point of view. Formulations in terms of stress resultants presented in [3,4] were discussed and extended to include viscoplastic material response by introducing rate equations for the evolution of the finite inelastic deformations. Special attention was given to the objectivity of the rates and to the form of the plastic flow potential. An alternative one dimensional formulation, obtained by introducing a kinematic constraint and numerically integrating over the cross section of the beam, was also presented. The effect of warping, which arises as a result of shear deformation, was considered in both formulations using the kinematic assumption proposed in [3,4].

A numerical algorithm for the time dependent problem was presented, inspired by the one advocated by Hughes and Taylor [7], but modified so that the numerically integrated nonlinear rate equations are "exactly" satisfied at each iteration of the Newton-Raphson scheme. The implications of the formulations discussed in this paper were illustrated through a comprehensive set of numerical examples.

Acknowledgements - The authors thank Professor J. M. Kelly for advice offered during the execution of this research. Support for the second author was provided by Professor E. P. Popov under a grant from the National Science Foundation (Grant No. CEE 81-07217). This support is gratefully acknowledged. The opinions expressed in this paper are those of the authors and do not necessarily reflect the views of NSF.

REFERENCES

[1] Antman, S. S., "The Theory of Rods," in **Handbuch der Physik** , Vol. VIa/2, Springer-Verlag, Berlin, 1972.

[2] Naghdi, P. M., "The Theory of Shells," in **Handbuch der Physik** , Vol. VIa/2, Springer-Verlag, Berlin, 1972.

[3] Simo, J. C., "Some Bifurcation Topics in Nonlinear Elastostatics," *Ph.D. Dissertation,* University of California, Berkeley, 1982.

[4] Simo, J. C., "A Consistent Formulation of Nonlinear Theories of Elastic Beams and Plates," *Report No. UCB/SESM-82/06,* University of California, Berkeley, 1982.

[5] Sokolnikoff, I. S., **Mathematical Theory of Elasticity** , McGraw-Hill, New York, 1956.

[6] Cowper, G. R., "The Shear Coefficient in Timoshenko's Beam Theory," *J. Appl. Mech.,* Vol. 33 (6), 1966.

[7] Hughes, T. J. R., and R. L. Taylor, "Unconditionally Stable Algorithms for Quasi-Static Elasto/Viscoplastic Finite Element Analysis," *Computers and Structures* , Vol. 8, 1978.

[8] Pinsky, P. M., and R. L. Taylor, "A Finite Deformation Formulation for Elasto/Viscoplastic Beam Structures," in *Computational Methods in Nonlinear Mechanics* , J.T. Oden, ed., North-Holland Publishing Co., Northtrop, Netherlands, 1980.

[9] Marsden, J. and T. J. R. Hughes, "Topics in the Mathematical Foundations of Elasticity" *Nonlinear Analysis and Mechanics: Heriot-Watt Symposium* , Vol. II, R.J. Knops, ed., Research Notes in Mathematics Vol. 27, Pitman, 1978.

[10] Klingenberg, W., **A Course in Differential Geometry** , Springer-Verlag, Berlin, 1976.

[11] Kantorovich, L. V. and V. I. Krylov, **Approximate Methods of Higher Analysis** , Interscience, New York, 1962.

[12] Green, A. E. and P. M. Naghdi, "A Note on Invariance Under Superposed Rigid Body Motions," *Journal of Elasticity,* Vol. 9 (1), 1979.

[13] Drucker, D. C., "The Effect of Shear on the Plastic Bending of Beams," *J. Appl. Mech.,* Vol. 23 (4), 1956.

[14] Neal, B. G., "The Effect of Shear and Normal Forces on the Fully Plastic Moment of a Beam of Rectangular Cross Section," *J. Appl. Mech.,* Vol. 23 (2), 1961.

[15] Neal, B. G., "Effect of Shear Force on the Fully Plastic Moment of an I-Beam," *J. Mech. Engng. Sci.,* Vol. 3 (3), 1961.

[16] Neal, B. G., "Effect of Shear and Normal Forces on the Fully Plastic Moment of and I-Beam," *J. Mech. Eng. Sci.,* Vol. 3 (3), 1961.

[17] Zienkiewicz, O. C., **The Finite Element Method** , Third Edition, McGraw-Hill, New York, 1977.

[18] Ciarlet, P. G. **The Finite Element Method for Elliptic Problems** , North Holland Publishers Co., 1978.

[19] Green, A. E., and P. M. Naghdi, "Some Remarks on Elastic-Plastic Deformation at Finite Strain," *Int. J. Engng. Sci.,* Vol. 9, 1971.

[20] Perzyna, P., "Fundamental Problems in Viscoplasticity," in *Advances in Applied Mechanics,* Vol. 9, 1966.

[21] Ortiz, M. "Topics in Constitutive Theory for Inelastic Solids," *Ph.D. Dissertation,* University of California, Berkeley, 1981.

[22] Simo, J. C. and J. M. Kelly, "Two-dimensional Finite Elasticity Analysis of the Stability of Multilayer Elastomeric Bearings," *Report No. UCB/SESM-81/06,* University of California, Berkeley, 1981.

[23] Simo, J. C. and R. L. Taylor, "Penalty Formulations for Incompressible Nonlinear Elastostatics," *Computer Methods in Applied Mechanics and Engineering,* Vol. 35, 1982.

[24] DaDeppo, D. A., and R. Schmidt, "Instability of Clamped-Hinged Circular Arches Subjected to a Point Load," *Trans. Am. Soc. Mech. Eng.,* ASME, Vol. 97 (3), 1975.

[25] Plantema, F. **The Bending and Buckling of Sandwich Beams Plates and Shells** , John Wiley and Sons, Englewood, New Jersey, 1966.

[26] Haringx, J. A., "On Highly Compressive Helical Springs and Rubber Rods and Their Applications to Free Mountings," Parts I,II,III, *Philips Res. Rep.* Vols. 3, 401 (1948), 4, 49 (1949), 4, 206 (1942).

[27] Gent, A. N., "Elastic Stability of Rubber Compression Springs," *J. Mech. Eng. Sci.,* Vol. 6 (4), 1964.

[28] Schapery, R. A. and D. L. Skala, "Elastic Stability of Elastomeric Columns," *Int. J. Solids Structures,* Vol. 12, 1976.

[29] Timoshenko, S. P. and J. N. Gere, **Theory of Elastic Stability** , McGraw-Hill, New York, 1951.

[30] Ciarlet, P. G., "A Justification of the Von Karman Equations," *Arch. Rat. Mech. Anal.,* Vol. 73, 1980.

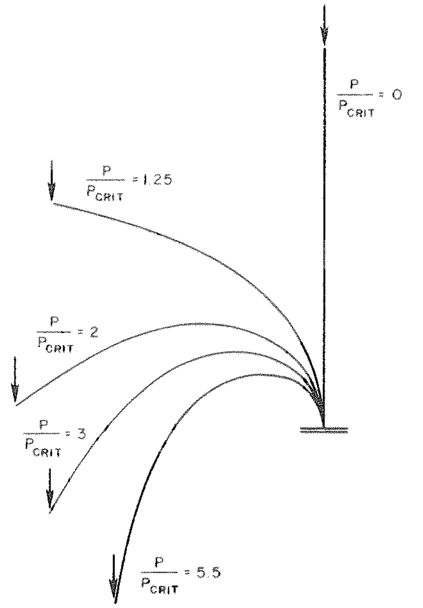

Fig. 4 Post-Buckling of an Euler Column.

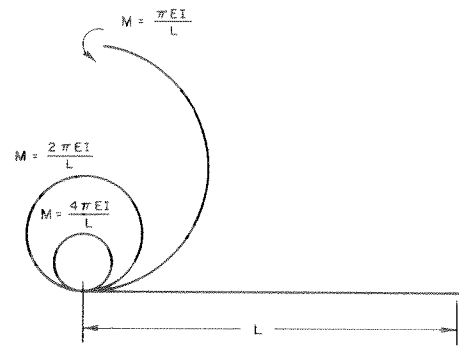

Fig. 5 Pure Bending of an Euler Beam.

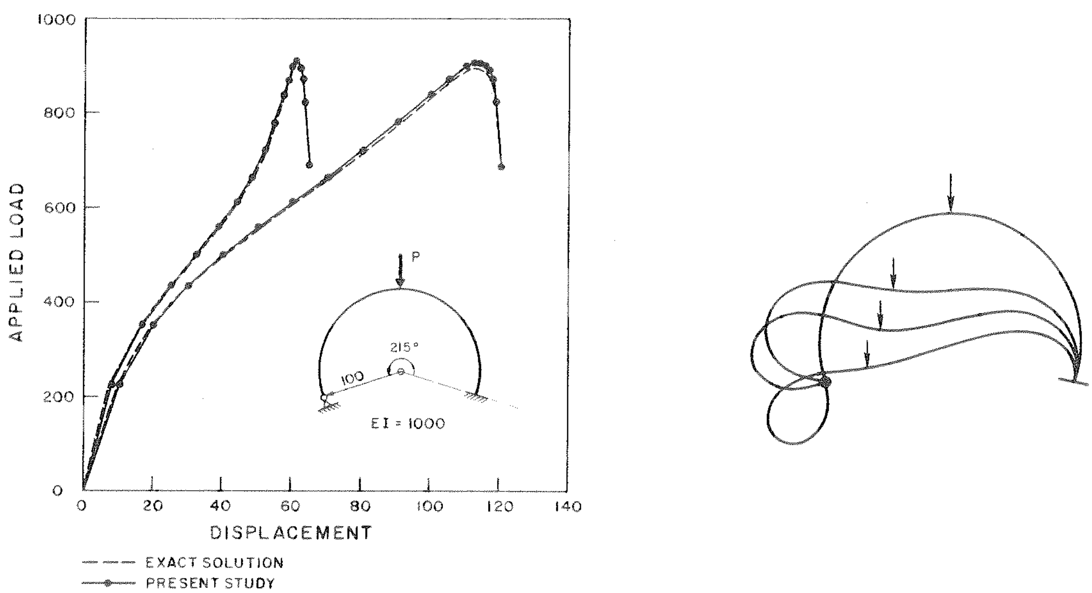

Fig. 6 Buckling of a Fixed-Hinged Circular Arch

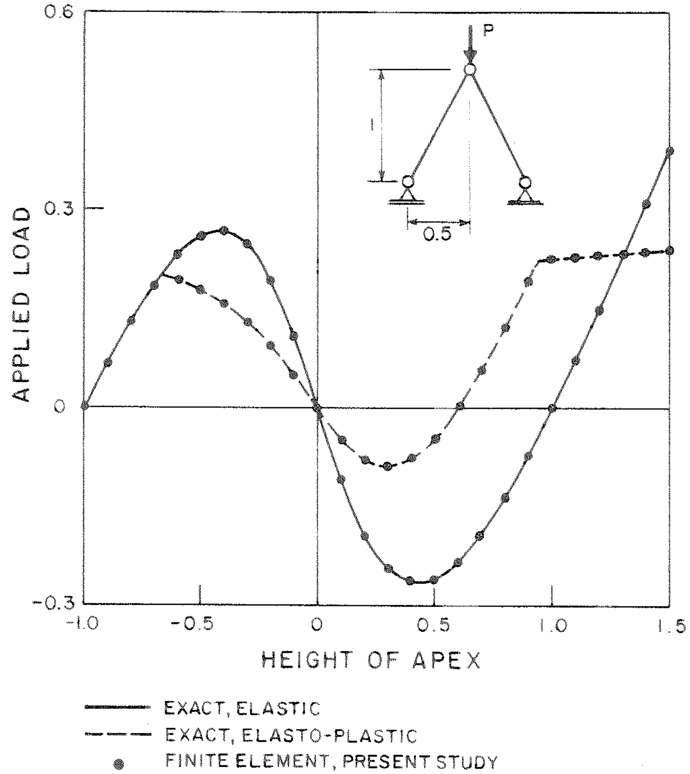

Fig. 7 Snap-Through of a Three Hinged Arch

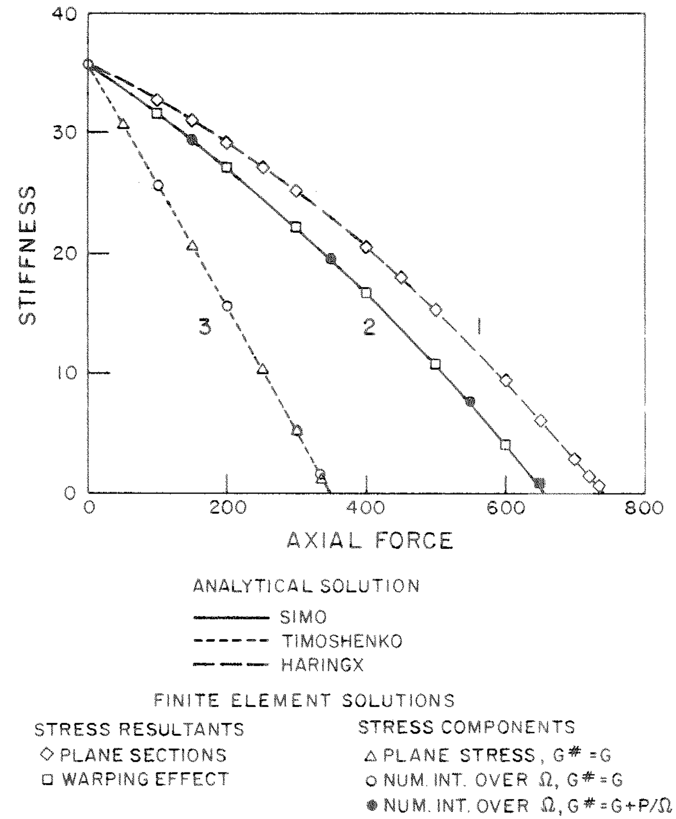

Fig. 8 Buckling of a Beam Flexible in Shear

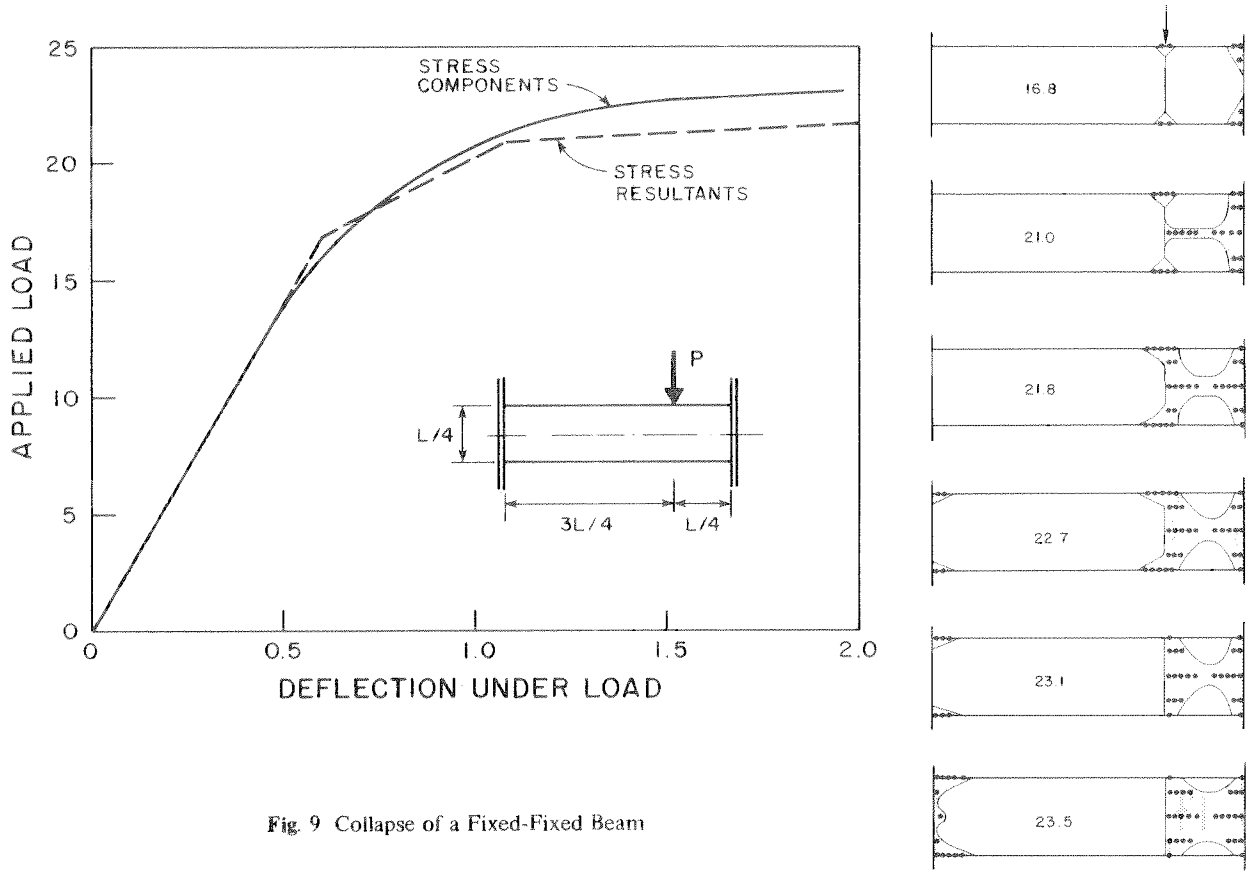

Fig. 9 Collapse of a Fixed-Fixed Beam

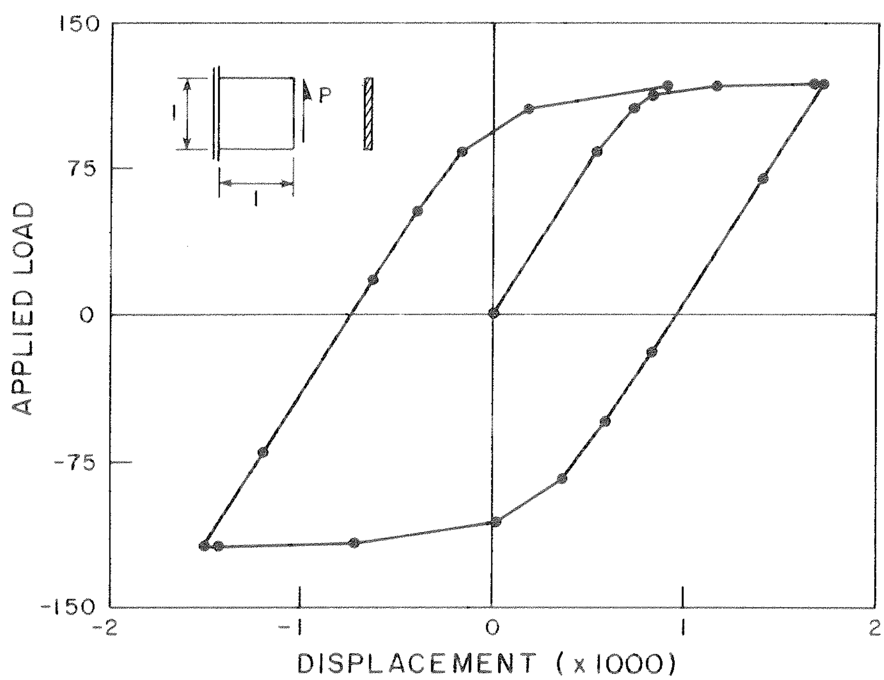

Fig. 10 Cyclically Loaded Rectangular Cantilever Beam

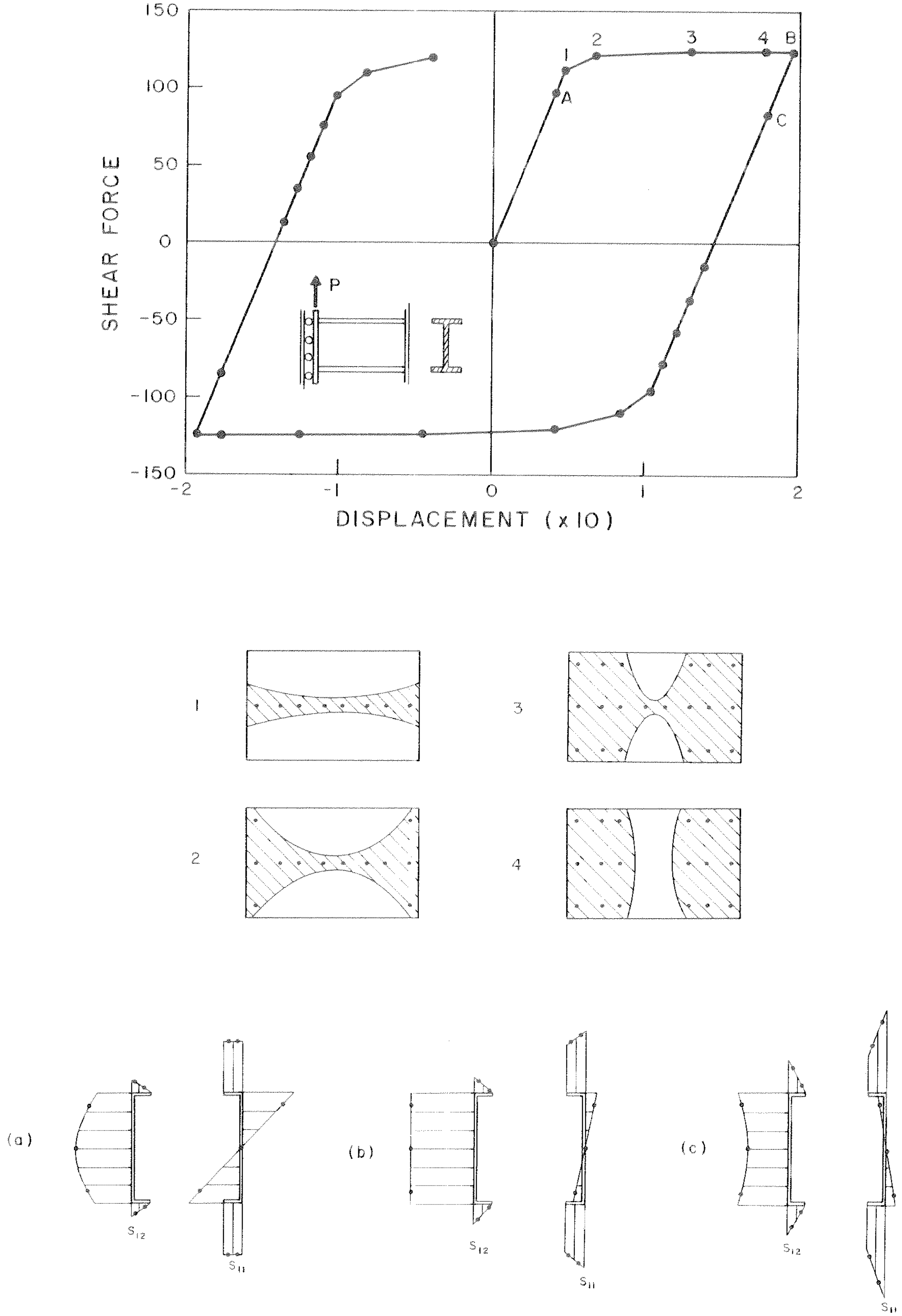

Fig. 11 Cyclically Loaded Fixed-Fixed I-Beam

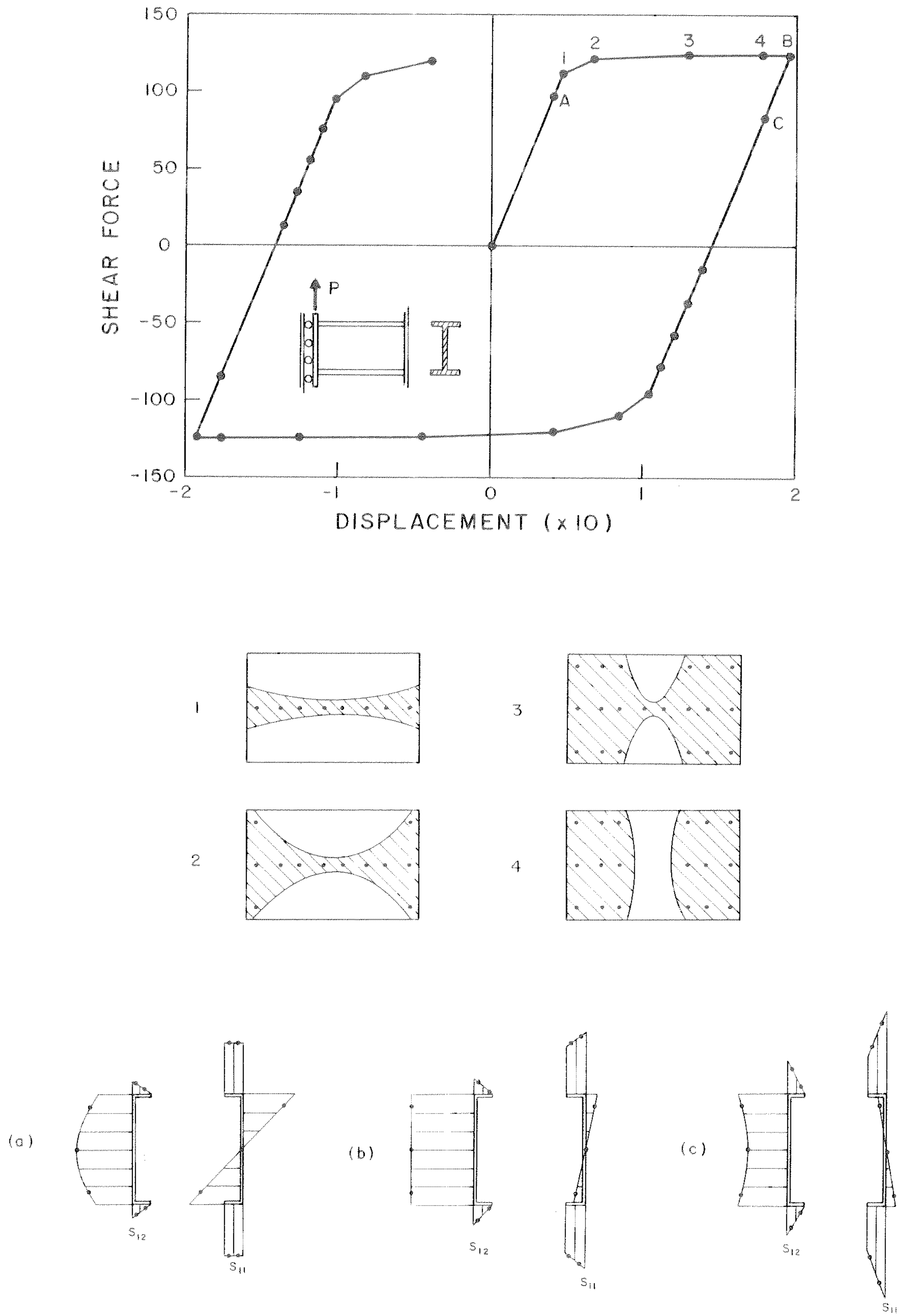

Fig. 11 Cyclically Loaded Fixed-Fixed I-Beam